Causal link between n-3 polyunsaturated fatty acid deficiency and motivation deficits

Fabien Ducrocq, Roman Walle, Andrea Contini, Asma Oummadi, Baptiste Caraballo, Suzanne van Der Veldt, Marie-Lou Boyer, Frank Aby, Tarson Tolentino-Cortez, Jean-Christophe Helbling, et al.

Causal link between n-3 Polyunsaturated Fatty Acid deficiency and motivation deficits

Fabien Ducrocq[1], Roman Walle[1], Andrea Contini[1], Asma Oummadi[1], Baptiste Caraballo[1], Suzanne van der Veldt [1], Marie-Lou Boyer[1], Frank Aby[1], Tarson Tolentino-Cortez[2], Jean-Christophe Helbling[1], Lucy Martine[3], Stéphane Grégoire[3], Stéphanie Cabaret[3], Sylvie Vancassel[1], Sophie Layé[1], Jing Xuan Kang[4], Xavier Fioramonti[1], Olivier Berdeaux[3], Gabriel Barreda-Gómez[2], Elodie Masson[3], Guillaume Ferreira[1], David W.L. Ma[5], Clementine Bosch-Bouju[1], Véronique De Smedt-Peyrusse[1], Pierre Trifilieff[1]

[1]Univ. Bordeaux, INRAE, Bordeaux INP, NutriNeuro, F-33000, Bordeaux, France

[2]Research department, IMG Pharma Biotech S.L., BIC Bizkaia (612), 48160-Derio, Spain

[3]Centre des Sciences du Goût et de l'Alimentation, AgroSup Dijon, CNRS, INRAE, Université Bourgogne Franche-Comté, F-21000 Dijon, France.

[4]Laboratory for Lipid Medicine and Technology, Massachusetts General Hospital and Harvard Medical School, Boston, MA 02129, USA

[5]Department of Human Health and Nutritional Sciences, University of Guelph, 50 Stone Rd. E., Guelph, ON, Canada N1G2W1

Contact information: Pierre Trifilieff (Lead contact) or Fabien Ducrocq

INRA, UMR 1286, Laboratoire NutriNeuro, Université de Bordeaux, Batiment UFR Pharmacie - 2eme Tranche - 2eme Etage – CC34, 146 rue Léo Saignat, 33076 BORDEAUX Cedex - France.

pierre.trifilieff@inrae.fr; fabien.ducrocq1989@gmail.com

Phone: +33557571248

SUMMARY

Reward-processing impairment is a common symptomatic dimension of several psychiatric disorders. However, whether the underlying pathological mechanisms are common is unknown. Herein, we asked if the decrease in the n-3 Polyunsaturated Fatty Acids (PUFAs) lipid species, consistently described in these pathologies, could underlie reward-processing deficits. We show that reduced n-3 PUFA biostatus in mice leads to selective motivational impairments. Electrophysiological recordings revealed increased collateral inhibition of dopamine D2 receptor-expressing medium spiny neurons (D2-MSNs) onto dopamine D1 receptor-expressing MSNs in the nucleus accumbens, a main brain region for the modulation of motivation. Strikingly, transgenically preventing n-3 PUFA deficiency selectively in D2-expressing neurons normalizes MSNs collateral inhibition and enhances motivation. These results constitute the first demonstration of a causal link between a behavioral deficit and n-3 PUFA decrease in a discrete neuronal population and suggest that lower n-3 PUFA biostatus in psychopathologies could participate to the etiology of reward-related symptoms.

Keywords: n-3 PUFA, Motivation, Dopamine, Nucleus Accumbens, Medium Spiny Neurons

INTRODUCTION

Symptom-focused transdiagnostic approach is increasingly considered in psychiatric research in order to identify common pathological mechanisms for the improvement of treatment algorithms. In this context, avolition, defined as the decrease in the motivation to initiate and perform self-directed purposeful activities (Diagnostic and statistical manual of mental disorders : DSM-5), is a common symptom of several psychiatric disorders such as major depressive disorder (MDD), bipolar disorders (BP) and schizophrenia (SCZ), that remains largely resistant to current pharmaceutical treatments. Numerous evidence support that this behavioral endophenotype originates from alterations within the brain reward system (for review, Whitton et al., 2015). However, whether this common symptom relies on shared pathological mechanisms remains largely unclear.

A growing body of evidence suggests the existence of a relationship for SCZ, BP and MDD. Indeed, several common genetic variants and pattern of gene expression (Gandal et al., 2018; Witt et al., 2017), as well as environmental factors (Nestler et al., 2016) have been identified as risk factors for the etiology of these diseases. Notably, meta-analyses and cross-sectional, case-control studies have consistently revealed decreased levels of phospholipid-containing n-3 long-chain polyunsaturated fatty acids (n-3 PUFAs) in erythrocytes and/or plasma of patients at high risk or with SCZ (Alqarni et al., 2019; Hoen et al., 2013), BP (Clayton et al., 2008; Pottala et al., 2012) or MDD (Lin et al., 2010; McNamara et al., 2014 ; for review: Messamore and McNamara, 2016). This suggests that low n-3 PUFA biostatus coincides with, and may precede the initial onset of psychopathologies. Moreover, even though there are some discrepancies (Igarashi et al., 2010; Lalovic et al., 2007; Yao et al., 2000), some postmortem analyses revealed lower brain n-3 PUFA contents in psychiatric patients (Conklin et al., 2010; McNamara et al., 2007a, 2007b, 2008; Tatebayashi et al., 2012). However, the implication of such decrease in n-3 PUFA levels in the etiology of the diseases remains largely controversial, notably due to discrepant outcomes from clinical trials that evaluated the effect of dietary n-3 PUFA supplementation on psychiatric symptoms. Indeed, while some meta-analyses observed significant advantage of n-3 PUFA supplementation for MDD (Grosso et al., 2014; Sublette et al., 2011) or BP (Sarris et al., 2012), some reported modest benefits (Appleton et al., 2015). Similarly, in patients at risk for SCZ, a first follow-up study found reduced risk of progression to psychotic disorders after n-3 PUFA supplementation (Amminger et al., 2015) which failed to be reproduced in a multi-center clinical trial (McGorry et al., 2017). Nonetheless, these findings highlight that, if any, the neurostructural and neurochemical perturbations resulting from lower n-3 PUFA biostatus could be difficult to reverse with late supplementation. This is likely due to their

developmental origin (Amminger et al., 2015), in accordance with the strong developmental etiology of these psychiatric disorders (Owen and O'Donovan, 2017).

PUFAs are fatty acid species that contain two or more unsaturation in their carbon chain. They divide in two main species, depending on the position of the first unsaturation, on the 3rd or the 6th carbon for n-3 and n-6 PUFA families, respectively. PUFAs are main constituents of cell membrane phospholipids. They accumulate in the brain during *in utero* development and constitute roughly 30% of total brain lipids in adulthood, where they can modulate membrane properties, signaling pathways and cell metabolism (Bazinet and Layé, 2014). Preclinical models revealed that developmental n-3 PUFA deficiency disrupts neurogenesis and neuronal differentiation (Beltz et al., 2007; Calderon and Kim, 2004), synaptic pruning (de Velasco et al., 2012) and endocannabinoid-dependent plasticity (Lafourcade et al., 2011; Thomazeau et al., 2016). Functionally, gestational n-3 PUFA deficiency in rodents recapitulates some symptomatic dimensions of psychiatric disorders such as anxiety-like behaviors and cognitive deficits (Lafourcade et al., 2011; Larrieu et al., 2012, 2014; Maekawa et al., 2017). Concerning the reward system, perinatal n-3 PUFA deficiency until weaning potentiates reinforcing effects of sucrose (Auguste et al., 2018). Multigenerational n-3 PUFA deficiency has been shown to result in discrete alterations in several markers of dopamine transmission (for review, see Chalon, 2006) paralleled with mild instrumental learning deficits (Bondi et al., 2014). However, regarding these latter findings, it is difficult to rule out an implication of transmissible epigenetic effects of n-3 PUFA decrease. Nonetheless, all the aforementioned observations remain correlative and the causal links between central n-3 PUFA deficiency-induced neurobiological alterations and behavioral deficits remain to be established.

Herein, we focused on reward processing as a main common symptomatic dimension of psychiatric disorders in which decreased n-3 PUFA biostatus has been described. We show that n-3 PUFA deficiency from gestation to adulthood leads to selective motivational deficits in adulthood, accompanied by increased collateral inhibition of dopamine D2 receptor-expressing medium spiny neurons (D2-MSNs) onto D1 receptor-expressing MSNs (D1-MSNs) in the nucleus accumbens. Strikingly, using a unique transgenic model, we demonstrate that preventing n-3 PUFA deficiency selectively in dopamine D2-expressing neurons reverses alterations in collateral inhibition between MSNs and enhances motivational performance in n-3 PUFA deficient animals. This study establishes for the first time a causal link between PUFA alteration in a discrete neuronal population and behavioral deficits, and suggests that decreased n-3 PUFA biostatus could participate to the etiology of reward processing impairments in psychiatric disorders.

RESULTS

N-3 PUFA deficiency from gestation to adulthood selectively alters PUFA content in brain phospholipids

The efficacy of dietary manipulation to alter brain PUFA composition has been previously validated (Joffre et al., 2016) (see Table S1 for diet compositions). N-3 PUFA deficiency from gestation to adulthood had no effect on the proportions of phospholipid classes nor on cholesterol levels (Fig. 1A-B) measured by liquid chromatography (LC)-Corona or Gas Chromatography with flame ionization detection, respectively (Fig. S1A). We then analyzed the fatty acid composition of the 3 main phospholipid classes, namely, phosphatidylethanolamines (PE), phosphatidylcholine (PC) and sphingomyelin (SM) by LC coupled with mass spectrometry (LC-MS) (Fig. S1A). We first found that n-3 PUFA deficiency led to an overall decrease in the number of unsaturation due to a decrease in the relative abundance of phospholipids containing 6 unsaturation (40:6 and 38:6) in favor of phospholipids containing 4 or 5 unsaturation (38:4, 38:5 and 40:5) (Fig. 1C-D). This effect was mainly observed in PEs, the main reservoir of PUFAs, compared to PCs and SMs (Fig. 1C-D and Fig. S1B-E). Gas chromatography analysis revealed that this effect was mostly related to a decrease in the n-3 PUFA Docosahexaenoic acid (DHA, C22:6) – the main n-3 PUFA in the brain - and an increase in the n-6 PUFA Docosapentaenoic acid (DPA, C22:5) (Fig. 1E). We also observed a slight, though significant augmentation of the main n-6 PUFA arachidonic acid (AA, C20:4) (Fig. 1E). This led to whole-brain increase in n-6/n-3 ratio (Fig. 1F). These changes mostly resulted from the replacement of DHA by n-6 DPA in PEs, even though n-6 DPA was present in very little amounts in the brain of control animals (Fig. 1D-E, G). It is likely that such enrichment in n-6 DPA under n-3 PUFA deficiency reflects a compensatory mechanism that allows maintaining membrane integrity in terms of length of the phospholipid sn-2 acyl chains since DPA and DHA only differ by one unsaturation (see Table S2 for detailed brain lipidomic analyses).

N-3 PUFA deficiency leads to deficits in effort-based tasks in adulthood that can be prevented by perinatal supplementation

We next assessed the effect of n-3 PUFA deficiency on motivational processes and their potential reversibility by postnatal n-3 PUFA supplementation (Fig.2A). In its broadest sense, motivation can be defined as the process that energizes behavior in pursuit of a goal and relies on several parameters such as cost-benefit computation, vigor, or persistence (Salamone and Correa, 2012; Simpson and Balsam, 2016). In order to evaluate the impact of n-3 PUFA deficiency on these subcomponents of motivation, we used 2 operant conditioning paradigms, the progressive ratio

(PRx2) and the concurrent lever pressing/free-feeding tasks. These effort-based tasks assess the ability of animals to exert effort in face of increasing motivational demand, and to obtain a preferred reward in the presence of a less preferred, though freely-accessible food, respectively. Performances of n-3 PUFA deficient animals were similar to controls in low work requirement tasks (FR-RR) both in terms of amount of instrumental responses as well as press rate (Fig. 2B-C). However, they displayed consistent impairments in both effort-based tasks (Fig 2D-E and S2A). More specifically, we did not observe significant decrease in total lever-pressing or breakpoint, likely due to the fact that, in the PRx2 task, the large majority of lever pressing are generated within lower, less-demanding ratios (Fig. 2D and Fig. S2A). However, n-3 PUFA deficient animals stopped lever-pressing earlier as reflected by decreased session duration and "survival", 2 parameters classically used to assess the ability of animals to maintain effort (Bailey et al., 2016; Carvalho Poyraz et al., 2016; Donthamsetti et al., 2018; Filla et al., 2018; Gallo et al., 2018; Simpson et al., 2014). Importantly, there was no significant difference in press rates for a given ratio or overall press rates (Fig. 2D and Fig. S2A). These data suggest that, while instrumental vigor is spared, n-3 PUFA deficient animals display a selective deficit in the ability to maintain effort when the motivational demand becomes too high. A comparable deficit was also present in n-3 PUFA deficient females (Fig. S2B). In the concurrent lever pressing/free-feeding task, n-3 PUFA deficient animals displayed increased consumption of freely-accessible, less-preferred food at the expense of lever pressing for the preferred reward (Fig 2E). This difference in resource allocation towards low-effort alternative supports an impairment of cost-benefit computation in n-3 PUFA deficient animals (Salamone et al., 2018; Trifilieff et al., 2013). Interestingly, this resembles the motivational deficit characteristic of SCZ, BP and MDD, that has been shown to originate in part from a distortion of outcome anticipation and representation (Whitton et al., 2015). Importantly, neither the licking microstructures during consumption of the palatable reward (Fig. 2F), that allow assessing hedonic reactivity, palatability of the tastant and postingestive feedback mechanisms (Ducrocq et al., 2019), nor spontaneous locomotion were altered in n-3 PUFA deficient animals (data not shown). Altogether, these data support that the deficits in effort-based tasks in n-3 PUFA deficient animals are specifically related to impairments in motivational processes with no alteration of hedonic or motoric components.

In order to evaluate the developmental component of n-3 PUFA deficiency-induced motivational deficits, we assessed if supplementing n-3 PUFA deficient animals with n-3 long chain (LC)-PUFAs starting at birth or at weaning could reverse motivational deficits in adulthood. Whereas n-3 PUFA supplementation (fish oil, see Table S1) at P21 failed to reverse the motivational deficit, P0 supplementation rescued performance in the PRx2 task (Fig. 2G-H and Fig. S2C-D), suggesting that n-

3 PUFA deficiency during the perinatal period is critical for the development of neuronal networks controlling motivation.

Dopamine transmission *per se* is spared by n-3 PUFA deficiency

Dopamine transmission, and especially the mesolimbic pathway constituted by projections from the midbrain to the ventral striatum (or Nucleus Accumbens, NAc), is a main neuromodulatory system involved in motivational processes (Salamone and Correa, 2012; Trifilieff et al., 2013). To assess its functional integrity under n-3 PUFA deficiency, we challenged animals with amphetamine – which increases extracellular dopamine levels, particularly in the NAc - and evaluated the impact on motivational performance. Strikingly, the pro-motivational effect of amphetamine in the PRx2 task was blunted in n-3 PUFA deficient animals (Fig. 3A), suggesting that n-3 PUFA deficiency impacted mesolimbic dopamine transmission, as previously shown with multigenerational models (Bondi et al., 2014; Chalon, 2006). However, we did not detect any change neither in basal and amphetamine-induced dopamine release using microdialysis (Fig. 3B), nor in the expression levels of the dopamine transporter DAT and of the L-DOPA synthetizing enzyme tyrosine hydroxylase (TH) in the NAc (Fig. 3C and Fig. S3). These data suggested that the presynaptic component of mesolimbic dopamine transmission was spared in n-3 PUFA deficient animals. Moreover, expression of the two main dopamine receptors D1 and D2 was not significantly changed in the NAc of n-3 PUFA deficient animals (Fig. 3C and Fig. S3). Altogether, these data suggested that dopamine transmission *per se* was preserved in n-3 PUFA deficient animals, in contrast to what had been described in multigenerational models of deficiency (Bondi et al., 2014; Chalon, 2006).

N-3 PUFA deficiency enhances D2 receptor-dependent inhibitory inputs onto D1-MSNs.

Considering their central role in the modulation of motivation (Carvalho Poyraz et al., 2016; Natsubori et al., 2017; Soares-Cunha et al., 2016), we assessed the integrity of dopaminoceptive Medium Spiny Neurons (MSNs) – the main neuronal population of the striatum - in the NAc. Similarly to our findings on the whole brain (Fig. 1), n-3 PUFA deficiency strongly altered membrane PUFA composition in the striatum. However, we observed moderate though significant changes in the levels of cholesterol and some phospholipid species (Fig. S4A-K), supporting a unique sensitivity of the striatum to PUFA manipulations (see Table S3 for detailed striatal lipidomic analyses).

Functionality of MSNs of the NAc was assessed with whole-cell patch-clamp recording on acute brain slices containing the NAc from D1-GFP reporter mice (Fig. 4A). Basic intrinsic properties of both D1-MSNs (GFP-positive) and D2-MSNs (GFP-negative) were spared in n-3 PUFA deficient

animals (Fig. 4 B-J). Indeed, current-voltage and input-output curves were similar between n-3 PUFA deficient and control animals for both D1-MSNs and D2-MSNs (Fig. 4B-D). In accordance, membrane properties measured as resting membrane potential (RMP), rheobase, action potential (AP) threshold and input resistance, as well as spike properties such as delay to first spike and amplitude of action potential were similar in control and n-3 PUFA deficient animals for both MSN populations (Fig. 4E-J).

We further explored the firing capacity of MSNs in the NAc in response to electrical stimulation of the corpus callosum rostral to the NAc, which contains glutamatergic inputs originating from the prefrontal cortex, a main excitatory input onto the NAc (Fig. 5A). We found that the firing probability for a given excitatory post-synaptic potential (EPSP) slope (E-S coupling) resulting from electrical stimulation of glutamatergic afferents onto the NAc was decreased in D1-MSNs but not in D2-MSNs (Fig. 5B). This suggested a diminution in integrative properties of D1-MSNs to generate an action potential in response to extrinsic stimulation in n-3 PUFA deficient animals (Campanac and Debanne, 2008). This difference in E-S coupling in D1-MSNs between n-3 PUFA deficient and control animals was abolished under bath application of the $GABA_A$ antagonist Gabazine (Fig. 5C). These data confirm that GABA transmission is a main factor that regulates E-S coupling (Daoudal, 2003) and suggested that the decrease in E-S coupling in n-3 PUFA deficient animals resulted from an increase of GABAergic inputs onto D1-MSNs. In accordance, frequency of spontaneous inhibitory postsynaptic currents (sIPSCs) – but not excitatory postsynaptic currents (sEPSCs) – was significantly increased onto D1-MSNs, but not D2-MSNs, in n-3 PUFA deficient animals (Fig. 5D and S5A). This effect was preserved on miniature IPSCs (mIPSCs) (Fig. 5E and S5B). Finally, the increased inhibitory input onto D1-MSNs in n-3 PUFA deficient animals was further confirmed through an enhancement of extrasynaptic GABA-mediated tonic conductances, which have been demonstrated to strongly modulate neuronal excitability both *ex vivo* and *in vivo* (Borgkvist et al., 2015; Lemos et al., 2016; Maguire et al., 2014). Indeed, herein, we found that the effect of gabazine on $GABA_A$-mediated tonic conductances was more pronounced in D1-MSNs of n-3 deficient compared to control mice (Fig. S5C). Altogether, these data demonstrate an increase of inhibitory inputs onto D1-MSNs of the NAc in n-3 PUFA deficient animals.

It has been recently shown that a main GABAergic input onto D1-MSNs results from collateral projections of D2-MSNs and that this inhibitory transmission depends on the activity of dopamine D2 receptors (Dobbs et al., 2016; Lemos et al., 2016). Another main inhibitory input onto both MSN types originates from GABAergic interneurons, which do not seem to express the D2 receptor (Bertran-Gonzalez et al., 2008). Therefore, we tested whether the increase in GABA inputs onto D1-MSNs in n-3 PUFA deficient animals could be reversed by stimulation of D2 receptors that play a

main role in the control of GABA transmission by D2-MSNs (Dobbs et al., 2016; Lemos et al., 2016) (Fig. 5F). Application of the D2 receptor full agonist quinpirole normalized both E-S coupling (Fig. 5G) and sIPSCs frequency (Fig. 5H) in D1-MSNs from n-3 PUFA deficient animals, suggesting an increase in collateral inhibition of D2-MSNs onto D1-MSNs.

We next assessed the integrity of the dorsal part of ventral pallidum (VP), the main output structure of the NAc core in which virtually all neurons receive GABAergic projections from D2-MSNs while roughly half are contacted by D1-MSNs (Baimel et al., 2019; Kupchik et al., 2015). We performed patch-clamp recordings of VP neurons and found no difference neither in intrinsic properties, nor spontaneous firing (Fig. S5D). However, sIPSC frequency of dorsal VP neurons was decreased in n-3 PUFA deficient animals (Fig. S5E). In addition to local projections, the large majority of GABA inputs onto VP neurons originate from NAc MSNs (Root et al., 2015). Therefore, thanks to the specific Cre-dependent expression of a fluorescent reporter specifically in D2- or D1-expressing neurons, we evaluated the relative density of projections of each MSN population in the dorsal VP (Dobbs et al., 2019). Surprisingly, the relative density of projections originating from D2-expressing neurons was increased in the dorsal VP, while that from D1-expressing was unchanged, in n-3 PUFA deficient animals (Fig. S5F-G). Nonetheless, this alteration is unlikely to be the main mechanism that accounts for the motivational deficits in n-3 PUFA deficient animals since disinhibition of the dorsal VP neurons would rather lead to enhanced performance (Gallo et al., 2018). In contrast, the increased inhibitory tone we found onto D1-MSNs of the NAc would likely blunt motivational processes (Natsubori et al., 2017; Soares-Cunha et al., 2016). Altogether, these data therefore supported that motivational deficit in n-3 PUFA deficient animals could directly originate from enhanced collateral inhibitory input of D2-MSNs onto D1-MSNs in the NAc.

Selective rescue of PUFA levels in D2-expressing neurons reverses alterations of D1-MSN properties and increases motivational performance in n-3 PUFA deficient animals.

To further demonstrate the increase in collateral inhibition of D2-MSNs onto D1-MSNs in n-3 PUFA deficient animals, we asked whether preventing n-3 PUFA deficiency in D2-MSNs, could be sufficient to reverse the neurobiological alterations we observed in n-3 PUFA deficient animals. To do so, we used the “iFAT1 mouse”, a transgenic model that allows the Cre-dependent expression of the FAT1 enzyme (Clarke et al., 2014), a desaturase from c. elegans that converts n-6 PUFAs into n-3 PUFAs by the addition of one unsaturation (Fig. 6A-B). The Adora2a-Cre mouse is the model of choice for Cre-dependent recombination in D2-MSNs, selectively. However, the A2A receptor promoter is highly active at the periphery, notably in hepatocytes which are involved in the synthesis of LC-PUFAs from precursors (Alchera et al., 2015). Therefore, expression of the FAT1 enzyme by crossing the

iFAT1 mouse with Adora2a-Cre line would have resulted in a peripheral – and central - rescue of PUFA levels. Therefore, we crossed iFAT1 mice with Drd2(D2)-Cre animals (Fig. 6A).

Using reporter mice, we confirmed that such strategy was efficient to allow selective recombination in Cre-expressing MSNs in adulthood (Fig. S6A-B). In accordance with the prenatal activity of the D2 promoter in the striatum (Araki et al., 2007), Cre-dependent FAT1 mRNA expression was detectable prenatally as early as embryonic stages E17/E18 in the striatum – but not at E15 despite significant Cre expression (not shown) - (Fig. 6C), while still not detectable at P0 in the frontal cortex (Fig. S6C). At adulthood, we found a strong expression of FAT1 mRNA in the striatum, as well as a slight, though significant expression in the prefrontal cortex and the hypothalamus – brain regions in which the D2 promoter is known to be active (Beaulieu and Gainetdinov, 2011) – but not in the hippocampus (Fig. 6D). In the striatum, this resulted in a significant conversion of n-6 PUFAs into their n-3 PUFA equivalents (Fig. S6D). Importantly, at adulthood, PUFA composition of red blood cells was not altered in FAT1-expressing animals (Fig. S6E). This latter result supported the absence of PUFA conversion in peripheral organs involved in the biosynthesis and/or storage of LC-PUFAs. Accordingly, even though some slight Cre-independent expression of FAT1 was detectable in some peripheral organs, consistent with the previously-reported transgene “leakage” in the iFAT1 mouse (Clarke et al., 2014), we did not find any Cre-dependent expression of FAT1 in the pancreas, abdominal adipose tissue, liver or gut (Table S4).

FAT1 expression in D2-expressing neurons was sufficient to normalize both sIPSCs frequency and E-S coupling of MSNs in n-3 PUFA deficient animals (Fig. 6E). In order to ensure that these effects were due to selective rescue of the inhibitory inputs of D2-MSNs onto D1-MSNs, we expressed cre-dependent fluorescent inhibitory DREADDs (DIO-hM4DGi-mcherry) by viral-gene transfer in the NAc of n-3 PUFA deficient D2-Cre animals expressing (FAT1e), or not (FAT1ne), the FAT1 enzyme and performed patch-clamp recordings of D1-MSNs (non-fluorescent) (Fig. 6F-G). Of note, we found that, in D2-Cre mice, viral-mediated transduction of DREADDs led to very little, if any, expression in cholinergic interneurons (Fig. S6F-G), as previously described (Gallo et al., 2018). Application of the DREADD ligand Clozapine-N-Oxide (CNO) had no effect on basal properties or sEPSC frequency of D1-MSNs (Fig. S6H), but abolished the difference between FAT1 expressors (FAT1e) and FAT1 non-expressors (FAT1ne) n-3 PUFA deficient animals for both mIPSC frequency and E-S coupling of D1-MSNs (Fig. 6H). These data demonstrated that the decreased integrative properties of D1-MSNs under n-3 PUFA deficiency is the direct consequence of an increased collateral inhibition from D2-MSNs. Importantly, we did not find any alteration of dopamine release in the ventral striatum under FAT1 expression in D2-expressing neurons (Fig. S6I). These results confirmed the limited effect of n-3

PUFA deficiency on presynaptic mesolimbic dopamine transmission in our model and further support a main implication of D2-MSNs alterations in n-3 PUFA deficiency-induced motivational deficits.

Considering the pro-motivational role of D1-MSNs of the NAc core (Natsubori et al., 2017; Soares-Cunha et al., 2016), such an alteration of MSN network could likely account for motivational deficits in n-3 PUFA deficient animals. We therefore evaluated whether preventing n-3 PUFA decrease selectively in D2-expressing neurons would enhance performance in motivational tasks in n-3 PUFA deficient animals (Fig. 7A-B). Accordingly, n-3 PUFA deficient animals that expressed the FAT1 enzyme in D2-expressing neurons displayed a selective enhancement of performance in the progressive ratio task with no change in lever pressing under low motivational demand or pressing pattern (Fig. 7C and S7A). This effect was absent in control (i.e. non-deficient) mice (Fig. S7B). Strikingly, expression of the FAT1 enzyme in D1-expressing neurons – including D1-MSNs - had no effect on performance of n-3 PUFA deficient animals (Fig. 7D and S7C). Importantly, postnatal forebrain-specific expression of FAT1 mediated by αCAMK2 promoter-driven expression of the Cre recombinase – which includes MSNs (data not shown, Casanova et al., 2001) - failed to reverse the motivational deficit in n-3 PUFA deficient animals (Fig. S7D), confirming that the effects of n-3 PUFA deficiency on motivational performance result from perinatal effects (see discussion).

DISCUSSION

Decreased whole-body n-3 PUFA biostatus has been consistently described in MDD, BP and SCZ, three pathologies that share common symptoms, notably an alteration of reward-related processes. Even though these pathologies have been classically considered as distinct, an increasing approach in psychiatry is to favor symptomatic dimensions, avoiding categorical diagnostic boundaries, in order to identify transdiagnostic markers of common symptoms (Whitton et al., 2015). In this context, altogether, our data suggest that decreased n-3 PUFA biostatus could be involved in the etiology of motivational deficits and therefore constitute a biomarker for psychopathologies. Indeed, increasing evidence suggests that, rather than just a “loss of pleasure”, anhedonia, the core symptom of MDD, could originate from alterations in reinforcement learning, reward anticipation and willingness to exert efforts to obtain rewards, supporting a deficit in incentive processes (Whitton et al., 2015). Strikingly, individuals with MDD are less willing to exert effort to obtain potentially larger reward in the effort expenditure for rewards task (Treadway et al., 2012), which resembles what we observed in the effort-based choice task in n-3 PUFA deficient animals. Similarly, even though reward sensitivity is rather increased in manic phases of BP, patients in euthymic or depressive states display negative symptoms including avolition (Mancuso et al., 2015; Strauss et al.,

2016a; Thaler et al., 2013; Whitton et al., 2015). Avolition is also one of the main negative symptoms of SCZ and has been described as resulting from difficulty in representing rewarding experiences accurately (Strauss and Gold, 2012), leading to an inability to mobilize effort effectively (Whitton et al., 2015). The decreased ability to maintain effort in the progressive ratio paradigm and biased response towards low-effort alternatives in the effort-based choice task in n-3 PUFA deficient animals suggest that lower n-3 PUFA biostatus could participate to the etiology of reward processing symptoms. Clinical studies that assessed motivational deficits using progressive ratio or effort-based choice tasks reported a 20-45% decreased performance in SCZ patients under antipsychotics (Fervaha et al., 2013; Gold et al., 2013; Strauss et al., 2016b). Considering the well-known worsening effect of antipsychotics on negative symptoms, especially amotivation, the mild, though consistent deleterious effect of n-3 PUFA deficiency (12-15% decrease) holds symptomatic relevance, especially as a pre-symptomatic marker.

The impairment in reward processing in psychiatric disorders has been linked to alterations in dopamine transmission, which has been largely demonstrated to be involved in the modulation of motivation (Berke, 2018; Salamone and Correa, 2012). However, Positron Emission Tomography imaging, that allows measuring markers of dopamine transmission, such as receptor availability, dopamine synthesis and release, or transporter binding, so far failed to identify a common alteration in dopamine transmission *per se*. Indeed, such markers seem to be spared in patients with MDD (Cannon et al., 2009; Hirvonen et al., 2008, 2011; Montgomery et al., 2007), while dopaminergic abnormalities in BP have been related to lower dopamine transporter availability (Anand et al., 2011; Whitton et al., 2015), and the most robust finding in SCZ is elevated striatal dopamine levels (Weinstein et al., 2017). However, a common alteration in these pathologies is revealed by functional imaging studies that have consistently described abnormal reward-related activity of dopaminoceptive regions of the reward system, including the striatum, in patients with MDD (Bress et al., 2013; Pizzagalli et al., 2009), BP (Caseras et al., 2013; Mason et al., 2014) and SCZ (Howes et al., 2009; Morris et al., 2012). Strikingly, similarly to what has been described in psychiatric disorders, in n-3 PUFA deficient animals, we found no obvious difference in markers of dopamine transmission but rather an alteration in the functionality of dopaminoceptive MSN network in the NAc, which has been largely shown to be involved in the modulation of motivation (Carvalho Poyraz et al., 2016; Flanigan and LeClair, 2017; Gallo et al., 2018; Natsubori et al., 2017; Soares-Cunha et al., 2016; Trifilieff et al., 2013).

Our data strongly support that n-3 PUFA deficiency enhances the collateral inhibition of D2-MSNs onto D1-MSNs in the NAc, resulting in decreased excitability of D1-MSNs. The functional importance of this collateral connectivity between MSNs in the NAc has been recently unraveled. Even though it is still a matter of debate (Gallo et al., 2018), collateral inhibition of D2-MSNs onto D1-

MSNs has been proposed to be a main mechanism for the control of reward-related behaviors (Burke et al., 2017; Dobbs et al., 2016; Lemos et al., 2016). The dichotomic role of D1- and D2-MSNs of the NAc on instrumental responding and action initiation has been recently challenged (Natsubori et al., 2017; O'Connor et al., 2015; Soares-Cunha et al., 2016, 2019). However, knowing that activation of D1-MSNs facilitates operant responding in motivational tasks (Natsubori et al., 2017; Soares-Cunha et al., 2016), it is likely that enhanced inhibition from D2-MSNs onto D1-MSNs participates to decreased motivational performance in n-3 PUFA deficient animals. Accordingly, preventing n-3 PUFA decrease in D2-expressing neurons normalized collateral inhibition of D2-MSNs onto D1-MSNs, reversed D1-MSNs excitability and enhanced motivational performance in n-3 PUFA deficient, but not Ctrl, animals. Importantly, preventing n-3 PUFA decrease in D1-expressing neurons – which largely include D1-MSNs – did not have any effect on motivational performance, further supporting that the enhanced inhibitory output of D2-MSNs onto D1-MSNs is a main mechanism responsible for decreased motivation. Another main inhibitory output of D2-MSN projections in the VP and decreased excitability of D2-MSNs has been shown to enhance motivation through disinhibition of dorsal VP neurons activity (Gallo et al., 2018). In contrast, despite a slight increase of D2-MSN projections, our data show that, overall, in n-3 PUFA deficient animals, dorsal VP cells receive less inhibitory inputs, going against an implication of such alteration in the motivational deficit.

A caveat to our approach is the use of the D2-cre transgenic mouse model for driving the expression of FAT1 in D2-MSNs. Indeed, D2 promoter-driven cre-dependent recombination has been described in other neuronal subtypes than D2-MSNs such as a small subset of cholinergic interneurons in the striatum (Gallo et al., 2018), neurons of the midbrain (Khlghatyan et al., 2018), and clusters of cortical neurons (Khlghatyan et al., 2018). However, first, we found very little, if any, Cre-dependent recombination in cholinergic interneurons in the D2-Cre mouse as previously reported (Gallo et al., 2018). Second, dopamine release in the striatum seems to be spared in n-3 PUFA deficient animals, which we further confirmed by the absence of effect of FAT1 expression in D2-expressing neurons on dopamine transmission. Third, crossing the iFAT1 mouse with the D2-cre line indeed resulted in expression of FAT1 in cortical neurons at adulthood but not at P0. Yet, both dietary as well as transgenic manipulations support that the effect of n-3 PUFA deficiency results from perinatal effects (see below). It is thus unlikely that the effect of FAT1 expression in D2-expressing neurons on motivational performance results from PUFA rescue in cortical neurons. Altogether, our data therefore support that the motivational deficit in n-3 PUFA deficient animals mainly results from enhanced collateral inhibition of D2-MSNs onto D1-MSNs of the NAc.

The fact that the manipulation of PUFAs in D2-MSNs, but not D1-MSNs, results in functional alterations suggests a unique sensitivity of D2-MSNs to PUFA levels. One intriguing possibility, though difficult to test, would be that D1-MSNs and D2-MSNs display distinct lipid composition, making them

differentially sensitive to PUFA manipulations. Alternatively, it is possible that the unique vulnerability of D2-MSNs could be a consequence of D2 receptor-dependent signaling sensitivity to membrane PUFA manipulations. Indeed, studies of the prototypical class A GPCR rhodopsin demonstrate the existence of putative binding sites for the n-3 PUFA DHA (Grossfield et al., 2006; Palczewski et al., 2000; Soubias et al., 2006), allowing the preservation of optimal conformation and functionality of the receptor (Niu et al., 2004; Sánchez-Martín et al., 2013; SanGiovanni and Chew, 2005). However, whether such property is shared among class A GPCRs remains to be determined. Nonetheless, Molecular Dynamic simulation showed that membrane DHA levels modulate membrane diffusion rate of the D2 receptor (Guixà-González et al., 2016), and we obtained recent data demonstrating that membrane levels in DHA directly influence the activity of the D2 receptor (Jobin et al., *in preparation*). Therefore, it is possible that the increase in collateral inhibition from D2-MSNs onto D1-MSNs in n-3 PUFA deficient animals originates from an impairment of D2 receptor-dependent signaling. In accordance, D2 receptor-dependent signaling has been shown to be a main mechanism that regulates MSN collateral inhibition (Dobbs et al., 2016; Gallo et al., 2018; Lemos et al., 2016). Such an effect could result from an overall increase of D2-MSN projections since we found that the relative density of projections from D2-expressing neurons was increased in the dorsal VP. Further studies will be necessary to identify the cellular and molecular mechanisms at the origin of the unique sensitivity of D2-MSNs to PUFA manipulations.

Nonetheless, our data support that the effect of n-3 PUFA deficiency on motivational processes result from alterations taking place during the pre- and/or perinatal period. Indeed, conditional expression of FAT1 improved motivational performance in n-3 PUFA deficient animals when the expression of the Cre-recombinase was under the control of the D2-, but not the αCAMK2 promoter. Yet, consistent with the D2 promoter being active at embryonic stages (Araki et al., 2007), we found cre-dependent expression of FAT1 as early as E17/E18 in the striatum when iFAT1 mice were crossed with the D2-cre line. In contrast, in the αCAMK2-Cre line used in the current study, expression of the Cre recombinase occurs postnatally in the whole forebrain – including MSNs of the striatum (Casanova et al., 2001). It is therefore likely that perinatal rescue of PUFAs by FAT1 expression in D2R-expressing neurons accounts for prevention of n-3 PUFA deficiency-induced neurobiological and behavioral alterations. In accordance, performances in the motivational PRx2 task were rescued when prenatal deficiency was followed by n-3 PUFA supplementation starting at birth, but not at weaning. Interestingly, the maturation of MSN networks has been shown to occur mostly during the perinatal period (Tinterri et al., 2018). It is therefore tempting to propose that the impact of n-3 PUFA deficiency on motivational performance in adulthood originate from an alteration in the development/maturation of MSN networks.

This developmental effect of low n-3 PUFA biostatus is particularly relevant in the context of psychopathologies since they share strong developmental etiology (Owen and O'Donovan, 2017). The causes of the whole-body decrease in n-3 PUFA biostatus in SCZ, BP and MDD are unknown. Some studies report a correlation between functional outcomes and dietary n-3 PUFA consumption, but prevalence rates for these diseases as a function of dietary habits seem to be unaffected (Noaghiul and Hibbeln, 2003; Peet, 2004). However, a recent transcriptomic profiling study revealed a common pattern in fatty acid metabolic pathways in these diseases (Gandal et al., 2018), further supporting an implication of altered PUFA biostatus in the pathologies. Polymorphisms in several genes involved in PUFA metabolism such as Fatty Acid Binding Proteins (Hamazaki et al., 2016; Iwayama et al., 2010; Mocking et al., 2013) or phospholipases (Nadalin et al., 2008; Nurnberger et al., 2014; Su et al., 2010) have been described, suggesting that genetic predispositions could likely be responsible for n-3 PUFA decrease in psychiatric disorders. However, the causal link between such polymorphisms and the etiology of the diseases remain to be established. Nonetheless, it supports that the lower n-3 PUFA biostatus in the psychopathologies may contribute to the symptomatology and could constitute an early biomarker for reward-related symptoms, at least in a subset of individuals. In support of this idea, the increase and decrease in PE and PC species, respectively, in the striatum of n-3 PUFA deficient animals were particularly striking since a similar alteration in phospholipid species was described in the membranes of erythrocytes from a subgroup of SCZ patients that displayed the stronger positive and negative symptoms (Tessier et al., 2016).

Altogether, we demonstrate for the first time that manipulation of PUFA levels in a discrete neuronal population can causally result in behavioral deficit. Our data also support that n-3 PUFA deficiency during the perinatal period may be a main vulnerability mechanism for the development of reward processing deficits characteristic of psychiatric disorders such as MDD, BP and SCZ and could therefore constitute a transdiagnostic marker for these diseases. Further preclinical and clinical research is needed to identify the mechanisms responsible for such alteration in the pathologies in order to confirm the implication of lower n-3 PUFA biostatus in the etiology of psychiatric symptoms.

LIMITATIONS OF THE STUDY

In this study, we have established a causal link between developmental n-3 PUFA deficiency and behavioral impairments in two effort-based tasks in adulthood, with no change in hedonic reactivity and motoric abilities. This supports a selective motivational deficit in n-3 PUFA deficient animals, the PRx2 task revealing blunted ability to maintain effort, while the lever pressing/free feeding paradigm supports a propensity to choose low effort/low gain options at the expense of more effortful but larger rewards. However, further work is needed to identify which precise processes, such as

incentive salience, cost/benefit computation and/or reward prediction error are actually perturbed in n-3 PUFA deficient animals.

Moreover, we demonstrated that transgenically preventing n-3 PUFA deficiency selectively in D2-expressing neurons restores collateral inhibition of D2-MSNs onto D1-MSNs in the NAc on one hand and enhances performance in motivational tasks in n-3 PUFA deficient animals on the other hand. However, additional work will be required to ensure that this latter behavioural effect is directly and selectively related to the restoration of D2-MSN functionality in the NAc.

Finally, we show that D2-MSNs display a unique sensitivity to PUFA manipulations. However, an intriguing question remains unanswered: what are the cellular and molecular bases of such specific vulnerability?

STAR+METHODS

Detailed methods are provided in the online version of this paper and include the following:

- Key resources table
- Experimental model and subject details
- Methods details
    - Behavioral procedures
    - Lipid analyses
    - Electrophysiology
    - Stereotaxic Surgeries (microdialysis and viral injections)
    - High-Performance Liquid Chromatography
    - Immunohistochemistry / Microscopy
    - Western blot / Quantitative real-time PCR (q-PCR)
- Quantification and statistical analysis

Supplemental information: Supplemental Information includes seven figures and six tables and can be found with this article.

Acknowledgments: We thank Leste-Lasserre T. and Doat H. from the transcriptomic platform of the Neurocentre Magendie, INSERM U1215, Université Bordeaux for RTqPCR experiments, the Biochemistry and Biophysics Platform of the Bordeaux Neurocampus at the Bordeaux University funded by the LABEX BRAIN (ANR-10-LABX-43), Bordeaux Imaging Center funded by ANR-10-INBS-04 for imaging, Céline Ducroix-Crépy (INRA UMR 1286) for genotyping and the staff from the animal facility of INRA UMR 1286 for animal care.

Authors contributions: FD, RW, CBB, VDP and PT designed research, FD, RW, AC, LM, SG, SC, AO, BC, SVDV, MLB, FA and TTC, performed research, FD, GBG, EM, GF, CBB, VDP and PT supervised research, FD, RW, AC, EM, SVDV, OB, GBG, CBB, VDP and PT analyzed data, JCH, XF, SV, SL, JXK, DWLM

provided expertise, reagents and material, FD, GF, CBB and PT wrote the manuscript. All authors edited and approved the manuscript.

Funding: This study was supported by INRA and University of Bordeaux; Idex Bordeaux "chaire d'installation" (ANR-10-IDEX-03-02) (PT), NARSAD Young Investigator Grants from the Brain and Behavior Foundation (PT and CBB), ANR "SynLip" (ANR-16-CE16-0022) (PT), Region Nouvelle Aquitaine 2014-1R30301-00003023 (PT) and 2015-1R30116-00005095 (SL); ANR "Obeteen" (ANR-15-CE17-0013) (GF); PRESTIGE-2017-2-0031 (AC); "Fondation pour la Recherche Médicale" SPF201809007095 (AC); French research ministry (FD and RW); Conseil Régional de Bourgogne Franche-Comté (PARI grant) (EM and OB), European Funding for Regional Economic Development (FEDER) (EM and OB), "Fondation de France/Fondation de l'oeil" (EM and OB).

Disclosure: The authors declares no competing interest

REFERENCES

Acar, N., Berdeaux, O., Grégoire, S., Cabaret, S., Martine, L., Gain, P., Thuret, G., Creuzot-Garcher, C.P., Bron, A.M., and Bretillon, L. (2012). Lipid Composition of the Human Eye: Are Red Blood Cells a Good Mirror of Retinal and Optic Nerve Fatty Acids? PLoS ONE *7*, e35102.

Alchera, E., Imarisio, C., Mandili, G., Merlin, S., Chandrashekar, B.R., Novelli, F., Follenzi, A., and Carini, R. (2015). Pharmacological Preconditioning by Adenosine A2a Receptor Stimulation: Features of the Protected Liver Cell Phenotype. BioMed Research International *2015*, 1–9.

Alqarni, A., Mitchell, T.W., McGorry, P.D., Nelson, B., Markulev, C., Yuen, H.P., Schäfer, M.R., Berger, M., Mossaheb, N., Schlögelhofer, M., et al. (2019). Comparison of erythrocyte omega-3 index, fatty acids and molecular phospholipid species in people at ultra-high risk of developing psychosis and healthy people. Schizophrenia Research.

Amminger, G.P., Schäfer, M.R., Schlögelhofer, M., Klier, C.M., and McGorry, P.D. (2015). Longer-term outcome in the prevention of psychotic disorders by the Vienna omega-3 study. Nature Communications *6*.

Anand, A., Barkay, G., Dzemidzic, M., Albrecht, D., Karne, H., Zheng, Q.-H., Hutchins, G.D., Normandin, M.D., and Yoder, K.K. (2011). Striatal dopamine transporter availability in unmedicated bipolar disorder: Striatal DAT in unmedicated bipolar disorder. Bipolar Disorders *13*, 406–413.

Appleton, K.M., Sallis, H.M., Perry, R., Ness, A.R., and Churchill, R. (2015). Omega-3 fatty acids for depression in adults. Cochrane Database of Systematic Reviews.

Araki, K.Y., Sims, J.R., and Bhide, P.G. (2007). Dopamine receptor mRNA and protein expression in the mouse corpus striatum and cerebral cortex during pre- and postnatal development. Brain Res. *1156*, 31–45.

Auguste, S., Sharma, S., Fisette, A., Fernandes, M.F., Daneault, C., Des Rosiers, C., and Fulton, S. (2018). Perinatal deficiency in dietary omega-3 fatty acids potentiates sucrose reward and diet-induced obesity in mice. Int. J. Dev. Neurosci. *64*, 8–13.

Bailey, M.R., Simpson, E.H., and Balsam, P.D. (2016). Neural substrates underlying effort, time, and risk-based decision making in motivated behavior. Neurobiology of Learning and Memory *133*, 233–256.

Baimel, C., McGarry, L.M., and Carter, A.G. (2019). The Projection Targets of Medium Spiny Neurons Govern Cocaine-Evoked Synaptic Plasticity in the Nucleus Accumbens. Cell Rep *28*, 2256-2263.e3.

Bartlett, E.M., and Lewis, D.H. (1970). Spectrophotometric determination of phosphate esters in the presence and absence of orthophosphate. Anal. Biochem. *36*, 159–167.

Bazinet, R.P., and Layé, S. (2014). Polyunsaturated fatty acids and their metabolites in brain function and disease. Nature Reviews Neuroscience *15*, 771–785.

Beaulieu, J.-M., and Gainetdinov, R.R. (2011). The Physiology, Signaling, and Pharmacology of Dopamine Receptors. Pharmacological Reviews *63*, 182–217.

Beltz, B.S., Tlusty, M.F., Benton, J.L., and Sandeman, D.C. (2007). Omega-3 fatty acids upregulate adult neurogenesis. Neuroscience Letters *415*, 154–158.

Berdeaux, O., Juaneda, P., Martine, L., Cabaret, S., Bretillon, L., and Acar, N. (2010). Identification and quantification of phosphatidylcholines containing very-long-chain polyunsaturated fatty acid in bovine and human retina using liquid chromatography/tandem mass spectrometry. Journal of Chromatography A *1217*, 7738–7748.

Berke, J.D. (2018). What does dopamine mean? Nature Neuroscience *21*, 787–793.

Bertran-Gonzalez, J., Bosch, C., Maroteaux, M., Matamales, M., Herve, D., Valjent, E., and Girault, J.-A. (2008). Opposing Patterns of Signaling Activation in Dopamine D1 and D2 Receptor-Expressing Striatal Neurons in Response to Cocaine and Haloperidol. Journal of Neuroscience *28*, 5671–5685.

Bondi, C.O., Taha, A.Y., Tock, J.L., Totah, N.K.B., Cheon, Y., Torres, G.E., Rapoport, S.I., and Moghaddam, B. (2014). Adolescent Behavior and Dopamine Availability Are Uniquely Sensitive to Dietary Omega-3 Fatty Acid Deficiency. Biological Psychiatry *75*, 38–46.

Borgkvist, A., Avegno, E.M., Wong, M.Y., Kheirbek, M.A., Sonders, M.S., Hen, R., and Sulzer, D. (2015). Loss of Striatonigral GABAergic Presynaptic Inhibition Enables Motor Sensitization in Parkinsonian Mice. Neuron *87*, 976–988.

Bress, J.N., Foti, D., Kotov, R., Klein, D.N., and Hajcak, G. (2013). Blunted neural response to rewards prospectively predicts depression in adolescent girls: Feedback negativity predicts depression. Psychophysiology *50*, 74–81.

Burke, D.A., Rotstein, H.G., and Alvarez, V.A. (2017). Striatal Local Circuitry: A New Framework for Lateral Inhibition. Neuron *96*, 267–284.

Bustin, S.A., Benes, V., Garson, J.A., Hellemans, J., Huggett, J., Kubista, M., Mueller, R., Nolan, T., Pfaffl, M.W., Shipley, G.L., et al. (2009). The MIQE Guidelines: Minimum Information for Publication of Quantitative Real-Time PCR Experiments. Clinical Chemistry *55*, 611–622.

Calderon, F., and Kim, H.-Y. (2004). Docosahexaenoic acid promotes neurite growth in hippocampal neurons. Journal of Neurochemistry *90*, 979–988.

Campanac, E., and Debanne, D. (2008). Spike timing-dependent plasticity: a learning rule for dendritic integration in rat CA1 pyramidal neurons: STDP and plasticity of dendritic integration. The Journal of Physiology *586*, 779–793.

Cannon, D.M., Klaver, J.M., Peck, S.A., Rallis-Voak, D., Erickson, K., and Drevets, W.C. (2009). Dopamine Type-1 Receptor Binding in Major Depressive Disorder Assessed Using Positron Emission Tomography and [11C]NNC-112. Neuropsychopharmacology *34*, 1277–1287.

Carvalho Poyraz, F., Holzner, E., Bailey, M.R., Meszaros, J., Kenney, L., Kheirbek, M.A., Balsam, P.D., and Kellendonk, C. (2016). Decreasing Striatopallidal Pathway Function Enhances Motivation by Energizing the Initiation of Goal-Directed Action. Journal of Neuroscience *36*, 5988–6001.

Casanova, E., Fehsenfeld, S., Mantamadiotis, T., Lemberger, T., Greiner, E., Stewart, A.F., and Schütz, G. (2001). A CamKIIalpha iCre BAC allows brain-specific gene inactivation. Genesis *31*, 37–42.

Caseras, X., Lawrence, N.S., Murphy, K., Wise, R.G., and Phillips, M.L. (2013). Ventral Striatum Activity in Response to Reward: Differences Between Bipolar I and II Disorders. American Journal of Psychiatry *170*, 533–541.

Chalon, S. (2006). Omega-3 fatty acids and monoamine neurotransmission. Prostaglandins, Leukotrienes and Essential Fatty Acids *75*, 259–269.

Chomczynski, P., and Sacchi, N. (2006). The single-step method of RNA isolation by acid guanidinium thiocyanate–phenol–chloroform extraction: twenty-something years on. Nature Protocols *1*, 581–585.

Clarke, S.E., Kang, J.X., and Ma, D.W.L. (2014). The iFat1 transgene permits conditional endogenous n-3 PUFA enrichment both in vitro and in vivo. Transgenic Research *23*, 489–501.

Clayton, E.H., Hanstock, T.L., Hirneth, S.J., Kable, C.J., Garg, M.L., and Hazell, P.L. (2008). Long-Chain Omega-3 Polyunsaturated Fatty Acids in the Blood of Children and Adolescents with Juvenile Bipolar Disorder. Lipids *43*, 1031–1038.

Conklin, S.M., Runyan, C.A., Leonard, S., Reddy, R.D., Muldoon, M.F., and Yao, J.K. (2010). Age-related changes of n-3 and n-6 polyunsaturated fatty acids in the anterior cingulate cortex of individuals with major depressive disorder. Prostaglandins, Leukotrienes and Essential Fatty Acids *82*, 111–119.

Daoudal, G. (2003). Long-Term Plasticity of Intrinsic Excitability: Learning Rules and Mechanisms. Learning & Memory *10*, 456–465.

Delpech, J.-C., Thomazeau, A., Madore, C., Bosch-Bouju, C., Larrieu, T., Lacabanne, C., Remus-Borel, J., Aubert, A., Joffre, C., Nadjar, A., et al. (2015). Dietary n-3 PUFAs Deficiency Increases Vulnerability to Inflammation-Induced Spatial Memory Impairment. Neuropsychopharmacology *40*, 2774–2787.

Diagnostic and statistical manual of mental disorders : DSM-5 (Fifth edition. Arlington, VA : American Psychiatric Publishing, [2013]).

Dobbs, L.K., Kaplan, A.R., Lemos, J.C., Matsui, A., Rubinstein, M., and Alvarez, V.A. (2016). Dopamine Regulation of Lateral Inhibition between Striatal Neurons Gates the Stimulant Actions of Cocaine. Neuron *90*, 1100–1113.

Dobbs, L.K., Kaplan, A.R., Bock, R., Phamluong, K., Shin, J.H., Bocarsly, M.E., Eberhart, L., Ron, D., and Alvarez, V.A. (2019). D1 receptor hypersensitivity in mice with low striatal D2 receptors facilitates select cocaine behaviors. Neuropsychopharmacology *44*, 805–816.

Donthamsetti, P., Gallo, E.F., Buck, D.C., Stahl, E.L., Zhu, Y., Lane, J.R., Bohn, L.M., Neve, K.A., Kellendonk, C., and Javitch, J.A. (2018). Arrestin recruitment to dopamine D2 receptor mediates locomotion but not incentive motivation. Molecular Psychiatry.

Ducrocq, F., Hyde, A., Fanet, H., Oummadi, A., Walle, R., De Smedt-Peyrusse, V., Layé, S., Ferreira, G., Trifilieff, P., and Vancassel, S. (2019). Decrease in Operant Responding Under Obesogenic Diet Exposure is not Related to Deficits in Incentive or Hedonic Processes: Reward Processing and Obesogenic Diet Exposure. Obesity *27*, 255–263.

Fervaha, G., Graff-Guerrero, A., Zakzanis, K.K., Foussias, G., Agid, O., and Remington, G. (2013). Incentive motivation deficits in schizophrenia reflect effort computation impairments during cost-benefit decision-making. Journal of Psychiatric Research *47*, 1590–1596.

Filla, I., Bailey, M.R., Schipani, E., Winiger, V., Mezias, C., Balsam, P.D., and Simpson, E.H. (2018). Striatal dopamine D2 receptors regulate effort but not value-based decision making and alter the dopaminergic encoding of cost. Neuropsychopharmacology *43*, 2180–2189.

Flanigan, M., and LeClair, K. (2017). Shared Motivational Functions of Ventral Striatum D1 and D2 Medium Spiny Neurons. The Journal of Neuroscience *37*, 6177–6179.

Gallo, E.F., Meszaros, J., Sherman, J.D., Chohan, M.O., Teboul, E., Choi, C.S., Moore, H., Javitch, J.A., and Kellendonk, C. (2018). Accumbens dopamine D2 receptors increase motivation by decreasing inhibitory transmission to the ventral pallidum. Nature Communications *9*.

Gandal, M.J., Haney, J.R., Parikshak, N.N., Leppa, V., Ramaswami, G., Hartl, C., Schork, A.J., Appadurai, V., Buil, A., Werge, T.M., et al. (2018). Shared molecular neuropathology across major psychiatric disorders parallels polygenic overlap. Science *359*, 693–697.

Gold, J.M., Strauss, G.P., Waltz, J.A., Robinson, B.M., Brown, J.K., and Frank, M.J. (2013). Negative Symptoms of Schizophrenia Are Associated with Abnormal Effort-Cost Computations. Biological Psychiatry *74*, 130–136.

Grossfield, A., Feller, S.E., and Pitman, M.C. (2006). A role for direct interactions in the modulation of rhodopsin by -3 polyunsaturated lipids. Proceedings of the National Academy of Sciences *103*, 4888–4893.

Grosso, G., Pajak, A., Marventano, S., Castellano, S., Galvano, F., Bucolo, C., Drago, F., and Caraci, F. (2014). Role of Omega-3 Fatty Acids in the Treatment of Depressive Disorders: A Comprehensive Meta-Analysis of Randomized Clinical Trials. PLoS ONE *9*, e96905.

Guixà-González, R., Javanainen, M., Gómez-Soler, M., Cordobilla, B., Domingo, J.C., Sanz, F., Pastor, M., Ciruela, F., Martinez-Seara, H., and Selent, J. (2016). Membrane omega-3 fatty acids modulate the oligomerisation kinetics of adenosine A2A and dopamine D2 receptors. Scientific Reports *6*.

Hamazaki, K., Maekawa, M., Toyota, T., Iwayama, Y., Dean, B., Hamazaki, T., and Yoshikawa, T. (2016). Fatty acid composition and fatty acid binding protein expression in the postmortem frontal cortex of patients with schizophrenia: A case–control study. Schizophrenia Research *171*, 225–232.

Hirvonen, J., Karlsson, H., Kajander, J., Markkula, J., Rasi-Hakala, H., Någren, K., Salminen, J.K., and Hietala, J. (2008). Striatal dopamine D2 receptors in medication-naive patients with major depressive disorder as assessed with [11C]raclopride PET. Psychopharmacology *197*, 581–590.

Hirvonen, J., Hietala, J., Kajander, J., Markkula, J., Rasi-Hakala, H., Salminen, J.K., Någren, K., Aalto, S., and Karlsson, H. (2011). Effects of antidepressant drug treatment and psychotherapy on striatal and thalamic dopamine $D_{2/3}$ receptors in major depressive disorder studied with [^{11}C]raclopride PET. Journal of Psychopharmacology *25*, 1329–1336.

Hoen, W.P., Lijmer, J.G., Duran, M., Wanders, R.J.A., van Beveren, N.J.M., and de Haan, L. (2013). Red blood cell polyunsaturated fatty acids measured in red blood cells and schizophrenia: A meta-analysis. Psychiatry Research *207*, 1–12.

Howes, O.D., Egerton, A., Allan, V., McGuire, P., Stokes, P., and Kapur, S. (2009). Mechanisms underlying psychosis and antipsychotic treatment response in schizophrenia: insights from PET and SPECT imaging. Curr. Pharm. Des. *15*, 2550–2559.

Igarashi, M., Ma, K., Gao, F., Kim, H.-W., Greenstein, D., Rapoport, S.I., and Rao, J.S. (2010). Brain lipid concentrations in bipolar disorder. Journal of Psychiatric Research *44*, 177–182.

Iwayama, Y., Hattori, E., Maekawa, M., Yamada, K., Toyota, T., Ohnishi, T., Iwata, Y., Tsuchiya, K.J., Sugihara, G., Kikuchi, M., et al. (2010). Association analyses between brain-expressed fatty-acid binding protein (*FABP*) genes and schizophrenia and bipolar disorder. American Journal of Medical Genetics Part B: Neuropsychiatric Genetics *153B*, 484–493.

Joffre, C., Grégoire, S., De Smedt, V., Acar, N., Bretillon, L., Nadjar, A., and Layé, S. (2016). Modulation of brain PUFA content in different experimental models of mice. Prostaglandins, Leukotrienes and Essential Fatty Acids (PLEFA) *114*, 1–10.

Johnson, A.W. (2018). Characterizing ingestive behavior through licking microstructure: Underlying neurobiology and its use in the study of obesity in animal models. International Journal of Developmental Neuroscience *64*, 38–47.

Khlghatyan, J., Quintana, C., Parent, M., and Beaulieu, J.-M. (2018). High sensitivity mapping of cortical dopamine D2 receptor expressing neurons.

Koehrer, P., Saab, S., Berdeaux, O., Isaïco, R., Grégoire, S., Cabaret, S., Bron, A.M., Creuzot-Garcher, C.P., Bretillon, L., and Acar, N. (2014). Erythrocyte Phospholipid and Polyunsaturated Fatty Acid Composition in Diabetic Retinopathy. PLoS ONE *9*, e106912.

Kupchik, Y.M., Brown, R.M., Heinsbroek, J.A., Lobo, M.K., Schwartz, D.J., and Kalivas, P.W. (2015). Coding the direct/indirect pathways by D1 and D2 receptors is not valid for accumbens projections. Nature Neuroscience *18*, 1230–1232.

Lafourcade, M., Larrieu, T., Mato, S., Duffaud, A., Sepers, M., Matias, I., De Smedt-Peyrusse, V., Labrousse, V.F., Bretillon, L., Matute, C., et al. (2011). Nutritional omega-3 deficiency abolishes endocannabinoid-mediated neuronal functions. Nature Neuroscience *14*, 345–350.

Lalovic, A., Levy, E., Canetti, L., Sequeira, A., Montoudis, A., and Turecki, G. (2007). Fatty acid composition in postmortem brains of people who completed suicide. J Psychiatry Neurosci *32*, 363–370.

Larrieu, T., Madore, C., Joffre, C., and Layé, S. (2012). Nutritional n-3 polyunsaturated fatty acids deficiency alters cannabinoid receptor signaling pathway in the brain and associated anxiety-like behavior in mice. Journal of Physiology and Biochemistry *68*, 671–681.

Larrieu, T., Hilal, L.M., Fourrier, C., De Smedt-Peyrusse, V., Sans N, Capuron, L., and Layé, S. (2014). Nutritional omega-3 modulates neuronal morphology in the prefrontal cortex along with depression-related behaviour through corticosterone secretion. Translational Psychiatry *4*, e437–e437.

Lemos, J.C., Friend, D.M., Kaplan, A.R., Shin, J.H., Rubinstein, M., Kravitz, A.V., and Alvarez, V.A. (2016). Enhanced GABA Transmission Drives Bradykinesia Following Loss of Dopamine D2 Receptor Signaling. Neuron *90*, 824–838.

Lin, P.-Y., Huang, S.-Y., and Su, K.-P. (2010). A Meta-Analytic Review of Polyunsaturated Fatty Acid Compositions in Patients with Depression. Biological Psychiatry *68*, 140–147.

Livak, K.J., and Schmittgen, T.D. (2001). Analysis of Relative Gene Expression Data Using Real-Time Quantitative PCR and the 2−ΔΔCT Method. Methods *25*, 402–408.

Madore, C., Nadjar, A., Delpech, J.-C., Sere, A., Aubert, A., Portal, C., Joffre, C., and Layé, S. (2014). Nutritional n-3 PUFAs deficiency during perinatal periods alters brain innate immune system and neuronal plasticity-associated genes. Brain, Behavior, and Immunity *41*, 22–31.

Maekawa, M., Watanabe, A., Iwayama, Y., Kimura, T., Hamazaki, K., Balan, S., Ohba, H., Hisano, Y., Nozaki, Y., Ohnishi, T., et al. (2017). Polyunsaturated fatty acid deficiency during neurodevelopment in mice models the prodromal state of schizophrenia through epigenetic changes in nuclear receptor genes. Translational Psychiatry *7*, e1229.

Maguire, E.P., Macpherson, T., Swinny, J.D., Dixon, C.I., Herd, M.B., Belelli, D., Stephens, D.N., King, S.L., and Lambert, J.J. (2014). Tonic Inhibition of Accumbal Spiny Neurons by Extrasynaptic α4βδ GABA $_A$ Receptors Modulates the Actions of Psychostimulants. The Journal of Neuroscience *34*, 823–838.

Mancuso, S.G., Morgan, V.A., Mitchell, P.B., Berk, M., Young, A., and Castle, D.J. (2015). A comparison of schizophrenia, schizoaffective disorder, and bipolar disorder: Results from the Second Australian national psychosis survey. J Affect Disord *172*, 30–37.

Mason, L., O'Sullivan, N., Montaldi, D., Bentall, R.P., and El-Deredy, W. (2014). Decision-making and trait impulsivity in bipolar disorder are associated with reduced prefrontal regulation of striatal reward valuation. Brain *137*, 2346–2355.

McGorry, P.D., Nelson, B., Markulev, C., Yuen, H.P., Schäfer, M.R., Mossaheb, N., Schlögelhofer, M., Smesny, S., Hickie, I.B., Berger, G.E., et al. (2017). Effect of ω-3 Polyunsaturated Fatty Acids in Young People at Ultrahigh Risk for Psychotic Disorders: The NEURAPRO Randomized Clinical Trial. JAMA Psychiatry *74*, 19.

McNamara, R.K., Jandacek, R., Rider, T., Tso, P., Hahn, C.-G., Richtand, N.M., and Stanford, K.E. (2007a). Abnormalities in the fatty acid composition of the postmortem orbitofrontal cortex of schizophrenic patients: Gender differences and partial normalization with antipsychotic medications. Schizophrenia Research *91*, 37–50.

McNamara, R.K., Hahn, C.-G., Jandacek, R., Rider, T., Tso, P., Stanford, K.E., and Richtand, N.M. (2007b). Selective Deficits in the Omega-3 Fatty Acid Docosahexaenoic Acid in the Postmortem Orbitofrontal Cortex of Patients with Major Depressive Disorder. Biological Psychiatry *62*, 17–24.

McNamara, R.K., Jandacek, R., Rider, T., Tso, P., Stanford, K.E., Hahn, C.-G., and Richtand, N.M. (2008). Deficits in docosahexaenoic acid and associated elevations in the metabolism of arachidonic acid and saturated fatty acids in the postmortem orbitofrontal cortex of patients with bipolar disorder. Psychiatry Research *160*, 285–299.

McNamara, R.K., Strimpfel, J., Jandacek, R., Rider, T., Tso, P., Welge, J.A., Strawn, J.R., and DelBello, M.P. (2014). Detection and treatment of long-chain omega-3 fatty acid deficiency in adolescents with SSRI-resistant major depressive disorder. PharmaNutrition *2*, 38–46.

Messamore, E., and McNamara, R.K. (2016). Detection and treatment of omega-3 fatty acid deficiency in psychiatric practice: Rationale and implementation. Lipids in Health and Disease *15*.

Mocking, R.J.T., Lok, A., Assies, J., Koeter, M.W.J., Visser, I., Ruhé, H.G., Bockting, C.L.H., and Schene, A.H. (2013). Ala54Thr Fatty Acid-Binding Protein 2 (FABP2) Polymorphism in Recurrent Depression: Associations with Fatty Acid Concentrations and Waist Circumference. PLoS ONE *8*, e82980.

Montgomery, A.J., Stokes, P., Kitamura, Y., and Grasby, P.M. (2007). Extrastriatal D2 and striatal D2 receptors in depressive illness: Pilot PET studies using [11C]FLB 457 and [11C]raclopride. Journal of Affective Disorders *101*, 113–122.

Morris, R.W., Vercammen, A., Lenroot, R., Moore, L., Langton, J.M., Short, B., Kulkarni, J., Curtis, J., O'Donnell, M., Weickert, C.S., et al. (2012). Disambiguating ventral striatum fMRI-related bold signal during reward prediction in schizophrenia. Molecular Psychiatry *17*, 280–289.

Morrison, W.R., and Smith, L.M. (1964). PREPARATION OF FATTY ACID METHYL ESTERS AND DIMETHYLACETALS FROM LIPIDS WITH BORON FLUORIDE--METHANOL. J. Lipid Res. *5*, 600–608.

Nadalin, S., Rubeša, G., Giacometti, J., Vulin, M., Tomljanović, D., Vraneković, J., Kapović, M., and Buretić-Tomljanović, A. (2008). BanI polymorphism of cytosolic phospholipase A2 gene is associated with age at onset in male patients with schizophrenia and schizoaffective disorder. Prostaglandins, Leukotrienes and Essential Fatty Acids *78*, 351–360.

Natsubori, A., Tsutsui-Kimura, I., Nishida, H., Bouchekioua, Y., Sekiya, H., Uchigashima, M., Watanabe, M., de Kerchove d'Exaerde, A., Mimura, M., Takata, N., et al. (2017). Ventrolateral Striatal Medium Spiny Neurons Positively Regulate Food-Incentive, Goal-Directed Behavior Independently of D1 and D2 Selectivity. The Journal of Neuroscience *37*, 2723–2733.

Nestler, E.J., Peña, C.J., Kundakovic, M., Mitchell, A., and Akbarian, S. (2016). Epigenetic Basis of Mental Illness. The Neuroscientist *22*, 447–463.

Niu, S.-L., Mitchell, D.C., Lim, S.-Y., Wen, Z.-M., Kim, H.-Y., Salem, N., and Litman, B.J. (2004). Reduced G Protein-coupled Signaling Efficiency in Retinal Rod Outer Segments in Response to *n* -3 Fatty Acid Deficiency. Journal of Biological Chemistry *279*, 31098–31104.

Noaghiul, S., and Hibbeln, J.R. (2003). Cross-National Comparisons of Seafood Consumption and Rates of Bipolar Disorders. American Journal of Psychiatry *160*, 2222–2227.

Nurnberger, J.I., Koller, D.L., Jung, J., Edenberg, H.J., Foroud, T., Guella, I., Vawter, M.P., and Kelsoe, J.R. (2014). Identification of Pathways for Bipolar Disorder: A Meta-analysis. JAMA Psychiatry *71*, 657.

O'Connor, E.C., Kremer, Y., Lefort, S., Harada, M., Pascoli, V., Rohner, C., and Lüscher, C. (2015). Accumbal D1R Neurons Projecting to Lateral Hypothalamus Authorize Feeding. Neuron *88*, 553–564.

Owen, M.J., and O'Donovan, M.C. (2017). Schizophrenia and the neurodevelopmental continuum:evidence from genomics. World Psychiatry *16*, 227–235.

Palczewski, K., Kumasaka, T., Hori, T., Behnke, C.A., Motoshima, H., Fox, B.A., Le Trong, I., Teller, D.C., Okada, T., Stenkamp, R.E., et al. (2000). Crystal structure of rhodopsin: A G protein-coupled receptor. Science *289*, 739–745.

Peet, M. (2004). International variations in the outcome of schizophrenia and the prevalence of depression in relation to national dietary practices: an ecological analysis. Br J Psychiatry *184*, 404–408.

Pizzagalli, D.A., Holmes, A.J., Dillon, D.G., Goetz, E.L., Birk, J.L., Bogdan, R., Dougherty, D.D., Iosifescu, D.V., Rauch, S.L., and Fava, M. (2009). Reduced Caudate and Nucleus Accumbens Response to

Rewards in Unmedicated Individuals With Major Depressive Disorder. American Journal of Psychiatry *166*, 702–710.

Pottala, J.V., Talley, J.A., Churchill, S.W., Lynch, D.A., von Schacky, C., and Harris, W.S. (2012). Red blood cell fatty acids are associated with depression in a case-control study of adolescents. Prostaglandins, Leukotrienes and Essential Fatty Acids *86*, 161–165.

Root, D.H., Melendez, R.I., Zaborszky, L., and Napier, T.C. (2015). The ventral pallidum: Subregion-specific functional anatomy and roles in motivated behaviors. Prog. Neurobiol. *130*, 29–70.

Salamone, J.D., and Correa, M. (2012). The Mysterious Motivational Functions of Mesolimbic Dopamine. Neuron *76*, 470–485.

Salamone, J.D., Steinpreis, R.E., McCullough, L.D., Smith, P., Grebel, D., and Mahan, K. (1991). Haloperidol and nucleus accumbens dopamine depletion suppress lever pressing for food but increase free food consumption in a novel food choice procedure. Psychopharmacology (Berl.) *104*, 515–521.

Salamone, J.D., Correa, M., Yang, J.-H., Rotolo, R., and Presby, R. (2018). Dopamine, Effort-Based Choice, and Behavioral Economics: Basic and Translational Research. Frontiers in Behavioral Neuroscience *12*.

Sánchez-Martín, M.J., Ramon, E., Torrent-Burgués, J., and Garriga, P. (2013). Improved Conformational Stability of the Visual G Protein-Coupled Receptor Rhodopsin by Specific Interaction with Docosahexaenoic Acid Phospholipid. ChemBioChem *14*, 639–644.

SanGiovanni, J.P., and Chew, E.Y. (2005). The role of omega-3 long-chain polyunsaturated fatty acids in health and disease of the retina. Progress in Retinal and Eye Research *24*, 87–138.

Sarris, J., Mischoulon, D., and Schweitzer, I. (2012). Omega-3 for Bipolar Disorder: Meta-Analyses of Use in Mania and Bipolar Depression. The Journal of Clinical Psychiatry *73*, 81–86.

Simpson, E.H., and Balsam, P.D. (2016). The Behavioral Neuroscience of Motivation: An Overview of Concepts, Measures, and Translational Applications. Curr Top Behav Neurosci *27*, 1–12.

Simpson, E.H., Winiger, V., Biezonski, D.K., Haq, I., Kandel, E.R., and Kellendonk, C. (2014). Selective Overexpression of Dopamine D3 Receptors in the Striatum Disrupts Motivation but not Cognition. Biological Psychiatry *76*, 823–831.

Soares-Cunha, C., Coimbra, B., Sousa, N., and Rodrigues, A.J. (2016). Reappraising striatal D1- and D2-neurons in reward and aversion. Neuroscience & Biobehavioral Reviews *68*, 370–386.

Soares-Cunha, C., de Vasconcelos, N.A.P., Coimbra, B., Domingues, A.V., Silva, J.M., Loureiro-Campos, E., Gaspar, R., Sotiropoulos, I., Sousa, N., and Rodrigues, A.J. (2019). Nucleus accumbens medium spiny neurons subtypes signal both reward and aversion. Mol. Psychiatry.

Soubias, O., Teague, W.E., and Gawrisch, K. (2006). Evidence for specificity in lipid-rhodopsin interactions. J. Biol. Chem. *281*, 33233–33241.

Staff, N.P., and Spruston, N. (2003). Intracellular correlate of EPSP-spike potentiation in CA1 pyramidal neurons is controlled by GABAergic modulation. Hippocampus *13*, 801–805.

Strauss, G.P., and Gold, J.M. (2012). A New Perspective on Anhedonia in Schizophrenia. American Journal of Psychiatry *169*, 364–373.

Strauss, G.P., Vertinski, M., Vogel, S.J., Ringdahl, E.N., and Allen, D.N. (2016a). Negative symptoms in bipolar disorder and schizophrenia: A psychometric evaluation of the brief negative symptom scale across diagnostic categories. Schizophrenia Research *170*, 285–289.

Strauss, G.P., Whearty, K.M., Morra, L.F., Sullivan, S.K., Ossenfort, K.L., and Frost, K.H. (2016b). Avolition in schizophrenia is associated with reduced willingness to expend effort for reward on a Progressive Ratio task. Schizophrenia Research *170*, 198–204.

Su, K.-P., Huang, S.-Y., Peng, C.-Y., Lai, H.-C., Huang, C.-L., Chen, Y.-C., Aitchison, K.J., and Pariante, C.M. (2010). Phospholipase A2 and Cyclooxygenase 2 Genes Influence the Risk of Interferon-α–Induced Depression by Regulating Polyunsaturated Fatty Acids Levels. Biological Psychiatry *67*, 550–557.

Sublette, M.E., Ellis, S.P., Geant, A.L., and Mann, J.J. (2011). Meta-Analysis of the Effects of Eicosapentaenoic Acid (EPA) in Clinical Trials in Depression. The Journal of Clinical Psychiatry *72*, 1577–1584.

Tatebayashi, Y., Nihonmatsu-Kikuchi, N., Hayashi, Y., Yu, X., Soma, M., and Ikeda, K. (2012). Abnormal fatty acid composition in the frontopolar cortex of patients with affective disorders. Translational Psychiatry *2*, e204–e204.

Tessier, C., Sweers, K., Frajerman, A., Bergaoui, H., Ferreri, F., Delva, C., Lapidus, N., Lamaziere, A., Roiser, J.P., De Hert, M., et al. (2016). Membrane lipidomics in schizophrenia patients: a correlational study with clinical and cognitive manifestations. Translational Psychiatry *6*, e906–e906.

Thaler, N.S., Strauss, G.P., Sutton, G.P., Vertinski, M., Ringdahl, E.N., Snyder, J.S., and Allen, D.N. (2013). Emotion perception abnormalities across sensory modalities in bipolar disorder with psychotic features and schizophrenia. Schizophr. Res. *147*, 287–292.

Thomazeau, A., Bosch-Bouju, C., Manzoni, O., and Layé, S. (2016). Nutritional n-3 PUFA Deficiency Abolishes Endocannabinoid Gating of Hippocampal Long-Term Potentiation. Cerebral Cortex bhw052.

Tinterri, A., Menardy, F., Diana, M.A., Lokmane, L., Keita, M., Coulpier, F., Lemoine, S., Mailhes, C., Mathieu, B., Merchan-Sala, P., et al. (2018). Active intermixing of indirect and direct neurons builds the striatal mosaic. Nat Commun *9*, 4725.

Treadway, M.T., Bossaller, N.A., Shelton, R.C., and Zald, D.H. (2012). Effort-based decision-making in major depressive disorder: A translational model of motivational anhedonia. Journal of Abnormal Psychology *121*, 553–558.

Trifilieff, P., Feng, B., Urizar, E., Winiger, V., Ward, R.D., Taylor, K.M., Martinez, D., Moore, H., Balsam, P.D., Simpson, E.H., et al. (2013). Increasing dopamine D2 receptor expression in the adult nucleus accumbens enhances motivation. Molecular Psychiatry *18*, 1025–1033.

de Velasco, P.C., Mendonça, H.R., Borba, J.M.C., Andrade da Costa, B.L. da S., Guedes, R.C.A., Navarro, D.M. do A.F., Santos, G.K.N., Faria-Melibeu, A. da C., Campello Costa, P., and Serfaty, C.A. (2012). Nutritional restriction of omega-3 fatty acids alters topographical fine tuning and leads to a delay in the critical period in the rodent visual system. Experimental Neurology *234*, 220–229.

Weinstein, J.J., Chohan, M.O., Slifstein, M., Kegeles, L.S., Moore, H., and Abi-Dargham, A. (2017). Pathway-Specific Dopamine Abnormalities in Schizophrenia. Biological Psychiatry *81*, 31–42.

Whitton, A.E., Treadway, M.T., and Pizzagalli, D.A. (2015). Reward processing dysfunction in major depression, bipolar disorder and schizophrenia: Current Opinion in Psychiatry *28*, 7–12.

Witt, S.H., Streit, F., Jungkunz, M., Frank, J., Awasthi, S., Reinbold, C.S., Treutlein, J., Degenhardt, F., Forstner, A.J., Heilmann-Heimbach, S., et al. (2017). Genome-wide association study of borderline personality disorder reveals genetic overlap with bipolar disorder, major depression and schizophrenia. Transl Psychiatry *7*, e1155.

Yao, J.K., Leonard, S., and Reddy, R.D. (2000). Membrane phospholipid abnormalities in postmortem brains from schizophrenic patients. Schizophr. Res. *42*, 7–17.

MAIN FIGURE TITLES AND LEGENDS

Fig.1: n-3 PUFA deficiency leads to alteration of brain lipid composition

(**A-F**) Whole brain lipid composition measured at adulthood. % of principal phospholipid (PL) families (PE: phosphatidylethanolamine, PC: phosphatidylcholine, PI: phosphatidyl-inositol, SM: sphingomyelin) (**A**) as well as the amount of cholesterol (**B**) were similar in Ctrl and n-3 PUFA deficient groups. (**C**) However the relative abundance of the number of unsaturation within the two main families of phospholipids (PE and PC) were changed with significant decrease of PL containing 6 unsaturation compensated mostly by an increase in PL containing 5 unsaturation in n-3 PUFA deficient animals. These changes were mainly occurring within PEs. Indeed (**D**) detailed analysis of fatty acyl chains (>1% of total PE in control group) revealed that PEs containing 6, 5 or 4 unsaturations were the main species altered by n-3 PUFA deficiency. (**E**) Analysis of the % of main PUFA species confirmed that the major changes occurred for PUFAs containing 6 or 5 unsaturation, Docosahexaenoic Acid (DHA; C22:6 n-3) and Docosa-pentaenoic Acid (DPA; C22:5 n-6,) that were decreased and increased, respectively. Arachidonic Acid (AA; C20:4) was significantly though slightly increased in n-3 PUFA deficient animals. Concerning the 2 precursors upstream of DHA, Eicosapentaenoic Acid (EPA; C20:5) was not detected, while Alpha-Linolenic Acid (ALA; C18:3) was not changed. (**F**) These alterations in PUFA species resulted in an overall increase of n-6/n-3 PUFA ratio in n-3 PUFA deficient animals. (**G**) Schematic representation of the major modifications induced by n-3 PUFA deficiency in brain phospholipids: PE C40:6 change into PE C40:5 by the replacement of DHA (C22:6 n-3) by DPA (C22:5 n-6) in the sn2 position. Data are means ± sem. **p<0.01 ; ***p<0.001. Ctrl: control group ; n-3 def: n-3 PUFA deficient group. Raw lipidomic data are described in table 3. For statistical details, see Table S5.

Fig.2: n-3 PUFA deficiency from gestation to adulthood leads to motivational deficit

(**A**) Experimental models of nutritional n-3 PUFA deficiency in mice from gestation to adulthood (1) and supplementation with LC n-3 PUFA at either P21 (2) or P0 (3). (**B-C**) N-3 PUFA deficient mice displayed similar lever pressing than control animals during fixed ratio and random ratio tasks (FR-RR) in the total amount of operant responses (**B**) and press rates during FR1, RR10 and RR20 sessions (C). (**D**) N-3 PUFA deficient mice had shorter session duration during the progressive ratio task (PRx2) (Left) and decreased “survival” (Middle), but did not differ from control group in term of press rate, plotted as a function of ratio requirement (Right). (**E**) In the concurrent lever pressing/free feeding task, n-3 PUFA deficient mice displayed lower lever presses for the reward but higher consumption of the freely available food. (**F**) Analyses of licking microstructures during consumption of the freely-available reward showed that total consumption, number of licks, number of bursts, number of licks per burst and bursts duration were similar between n-3 def and Ctrl. (**G**) N-3 supplementation starting at P21 did not impact session duration or “survival” in the PRx2 task. **(H**) However, n-3 supplementation starting at P0 abolished the decrease in “survival” in n-3 PUFA deficient animals in the PRx2 task. Data are means ± sem. *p<0.05, **p<0.01. Ctrl: control group ; n-3 def: n-3 PUFA

deficient group ; suppl P21: n-3 PUFA supplementation starting at postnatal day 21 and suppl P0: n-3 PUFA supplementation starting at postnatal day 0. For statistical details, see Table S5.

Fig.3: dopamine transmission is spared by n-3 PUFA deficiency

(**A**) While i.p. amphetamine at 1 mg/kg enhanced lever pressing in control animals, it has no effect in n-3 PUFA deficient animals. (**B**) Measure of basal and amphetamine-stimulated dopamine release in the nucleus accumbens by microdialysis. (**C**) Western blot analyses of major dopaminergic markers: DAT, TH, D2R and D1R in the NAc. Data are means ± sem. *p<0.05. Ctrl: control group ; n-3 def: n-3 PUFA deficient group. For statistical details, see Table S5.

Fig.4: n-3 PUFA deficiency does not affect basal intrinsic properties of medium spiny neurons in the nucleus accumbens core

(**A**) Whole cell patch clamp recording of D1-MSNs and D2-MSNs in the core part of the nucleus accumbens. Representative image of nucleus accumbens slices of a D1-EGFP mouse at low magnification (top) and high magnification under light transmission (middle) and epifluorescence (bottom). (**B**) Representative traces of voltage responses in D1-MSNs (green box) and D2-MSNs (purple box). Measures of current-voltage curves (**C**), input-output curves (**D**), resting membrane potential (**E**), Rheobase (**F**), AP threshold (**G**), membrane resistance (**H**), Delay to 1st spike (**I**) and AP amplitude (**J**) in D1-MSNs (top, green box) and D2-MSNs (bottom, purple box). Data are means ± sem. All ps>0.05. Ctrl: control group ; n-3 def: n-3 PUFA deficient group. For statistical details, see Table S5.

Fig.5: n-3 PUFA deficiency leads to decreased excitability of medium spiny neurons from the direct pathway (D1-MSN) through a D2R-dependent increase in GABA transmission

(A) Schematic representation of a mouse sagittal slice with the patch pipette located in the core part of the nucleus accumbens and the stimulating electrode located on the corpus callosum. **(B)** Measure of the E-S coupling in both D1-MSNs (left) and D2-MSNs (right) revealed a significant decrease in excitability in response to electrical stimulation in D1-MSNs, but not D2-MSNs in n-3 PUFA deficient mice. **(C)** This effect in D1-MSNs was abolished by application of the GABA-A receptor antagonist Gabazine (Gbz). (**D**) D1-MSNs in n-3 PUFA deficient animals displayed increase in spontaneous IPSCs (sIPSC) frequency. This effect was globally observed for all the amplitude measured in D1-MSNs. (left) Representative sIPSC traces, (middle) plot of sIPSC frequencies and (right) plot of sIPSCs frequency/amplitude in D1-MSNs. (**E**) Frequency of miniature IPSCs (mIPSCs) measured after application of TTX was increased in D1-MSNs of n-3 PUFA deficient animals, and statistically increased for events of 20-30 pA. (left) Representative mIPSC traces, (middle) plot of mIPSC frequency and (right) plot of mIPSCs frequency/amplitude in D1-MSNs. (**F**) Schematic representation of the putative inhibitory effect of quinpirole on GABA release from D2 receptor-containing GABAergic synapses innervating D1-MSNs. (**G**) The decrease in E-S coupling in D1-MSNs of n-3 PUFA deficient animals was abolished by application of the D2 receptor agonist quinpirole (Quin). (**H**) The difference in sIPSC frequency in D1-MSNs was abolished by application of quinpirole. This effect is observed for all sIPSC amplitude. (left) Representative sIPSC traces, (middle) sIPSC frequency and (right) plot of sIPSCs frequency/amplitude in D1-MSNs. Data are means ± sem. *p<0.05. Ctrl: control group ; n-3 def: n-3 PUFA deficient group. Gbz: gabazine ; Quin: quinpirole ; TTX: tetrodotoxine. For statistical details, see Table S5.

Fig.6: Preventing n-3 PUFA deficiency selectively in D2R-expressing neurons rescues the lateral inhibition of D2-MSNs onto D1-MSNs

(**A**) Schematic representation of the genetic strategy for expression of the FAT1 transgene in D2R-expressing neurons. (**B**) Representation of the enzymatic effect of the FAT1 enzyme. It specifically converts linoleic acid (LA) into α-linolenic acid (ALA), arachidonic acid (AA) into eicosapentaenoic acid

(EPA) and docosapentaenoic acid (DPA) into docosahexaenoic acid (DHA). (**C**) Cre-dependent FAT1 mRNA expression was not detectable prenatally at gestational day 15 (E15) but was detectable at gestational day 17/18 (E17/E18) and postnatal day 0 in the striatum (P0). (**D**) FAT1 expression in the striatum (Str), the prefrontal cortex (PFC), the hippocampus (HC) and the hypothalamus (HT) measured by RT-qPCR. The dashed line represents the level of expression of FAT1 in the non-inducible FAT1 mouse that expresses FAT1 ubiquitously. (**E**) Expression of FAT1 in D2R-expressing neurons tends to reverse the increase in sIPSC frequency and reverses the increase in E-S coupling in MSNs. (**F**) Schematic representation for the injection of the double-inverted open-reading frame (DIO) hM4Di-mCherry-carrying viral vector injection in the NAc core of n-3 deficient Drd2-Cre, FAT1e or FAT1ne mice. Sagittal slice showing that viral vector-mediated expression of hM4Di-mCherry is largely restricted to neurons of the NAc core with mCherry-positive terminal fields in the dlVP. (**G**) This strategy allows restricting the expression of the inhibitory DREADD to D2R-expressing neurons that express (FAT1e) or not (FAT1ne) the FAT1 enzyme and record non-fluorescent neurons, putative D1-MSNs of the NAc core. (**H**) Activation of the inhibitory DREADD by CNO application abolished the difference in mIPSC frequency (left) and E-S coupling (right) in D1-MSNs between FAT1e and FAT1ne n-3 PUFA deficient animals. Data are means ± sem. #p<0.1, *p<0.05, **p<0.01 and ***p<0.001. Ctrl: control group ; n-3 def: n-3 PUFA deficient group ; Cre+: Cre recombinase expression, Cre-: no expression of Cre recombinase ; FAT1+: FAT1 transgene carrier, FAT1-: FAT1 non-carrier ; FAT1e : FAT1 expression, FAT1ne : FAT1 no expression ; CNO : bath application of clozapine-N-oxide. For statistical details, see Table S5.

Fig.7: Preventing n-3 PUFA deficiency selectively in D2R-expressing neurons enhances motivation
(**A-B**) Schematic representations of a mouse performing operant conditioning task (A) and of the genetic strategy for expression of the FAT1 transgene in D2-MSNs or D1-MSNs (B). (**C**) Expression of FAT1 in D2-expressing neurons in n-3 PUFA deficient animals enhanced session duration in the PRx2 task (left) as well as “survival” (middle) with no effect on press rate, plotted as a function of the ratio requirement (right). (**D**) Expression of FAT1 in D1-expressing neurons in n-3 PUFA deficient animals did not impact session duration (left), nor “survival” (middle) and press rate, plotted as a function of the ratio requirement (right) in the PRx2 task. Data are means ± sem. # p<0.1, *p<0.05. Ctrl: control group ; n-3 def: n-3 PUFA deficient group ; Cre+: Cre recombinase expression, Cre-: no expression of Cre recombinase ; FAT1+: FAT1 transgene carrier, FAT1-: FAT1 non-carrier. For statistical details, see Table S5.

STAR METHODS

Lead contact and materials availability

Further information and requests for resources and reagents should be directed to and will be fulfilled by the Lead Contact, Pierre Trifilieff (pierre.trifilieff@inrae.fr).

This study did not generate new unique reagents.

Experimental model and subject details

Mice were housed in groups of 4-10 animals in standard polypropylene cages and maintained in a temperature and humidity-controlled facility under a 12:12 light-dark cycle (8 :00 on) with *ad libitum* access to water and food. All animal care and experimental procedures were in accordance with the INRA Quality Reference System and to french legislations (Directive 87/148, Ministère de l'Agriculture et de la Pêche) and European (Directive 86/609/EEC). They followed ethical protocols approved by the Region Aquitaine Veterinary Services (Direction Départementale de la Protection des Animaux, approval ID: B33-063-920) and by the animal ethic committee of Bordeaux CEEA50. Every effort was made to minimize suffering and reduce the number of animals used.

The following mouse lines were used in this study: C57BL/6J from Janvier Laboratories (Robert Janvier, Le Genest St-Isle, France), D1-Cre (MMRC: 029178-UCD, strain code: Tg(Drd1-cre)EY262/Mmucd), D2-Cre (MMRC: 017263-UCD, strain code: Tg(Drd2-cre)ER44Gsat/Mmucd), CamK2-Cre (MGI: 2181426, strain code: Tg(Camk2a-cre)2Gsc), D1-EGFP (MGI: 3840915, strain code: Tg(Drd1-EGFP)X60Gsat), Cre-dependent tdTomato reporter mice (MGI: 104735, strain code: B6.Cg-Gt(ROSA)26Sor$^{tm9(CAG-tdTomato)Hze}$/J mice ; Jackson Laboratory) and iFAT1 (Provided by the Laboratory of Dr. David Ma (Clarke et al., 2014)). Heterozygous Cre-dependent tdTomato reporter mice were crossed with heterozygous D1-Cre, D2-Cre or CamK2-Cre males. Homozygous or heterozygous iFAT1 females were crossed to heterozygous D1-Cre, D2-Cre or CamK2-Cre males in order to generate double transgenic animals and the respective single transgenic and WT controls.

Female C57BL6/J mice were fed with isocaloric diets containing 5% fat with a high (n-3 def diet, see table S1) or low LA/ALA ratio (Ctrl diet, see table S1) across gestation and lactation and offspring were maintained under the same diet after weaning (Delpech et al., 2015; Madore et al., 2014), unless stated otherwise. A third diet, enriched in long chain PUFAs, was used in the supplementation experiments starting at P21 or P0 (Suppl diet, see table S1). All experiments were performed in adulthood.

Method details

Behavioral procedures

<u>Operant conditioning</u>

Apparatus

The operant chambers (Imétronic, France) had internal dimensions 30x40x36 (cm) and were located in a light- and sound- attenuating cabinet. Each operant chamber had two opaque panels at the right

and left walls and two clear Plexiglas panels at the back and front walls and was illuminated throughout all sessions with a houselight located at the top of the chamber. The chambers were equipped with two retractable levers (2x4x1 cm), only one of which was reinforced. Reinforced lever presses were indicated by a brief tone (65 db, 3000 Hz, 200 ms) and a cue light, mounted 8.5 cm above the lever. A drinking trough was positioned 4 cm above the grid floor at equidistance between the two levers. Milk was used as a reward, consisting of 10% sweetened condensed milk dissolved in water (3.25 Kcal/g), which was provided through 15µl drops. The number of presses on the reinforced lever and on the alternative lever were recorded, as well as the number of licks in the full or empty trough.

Procedures

One session (1 hour) was run each day, 5-7 days per week. Animals were food-restricted in order to maintain them at 85-90% of their *ad libitum* weight.

Pavlovian training: During 2-3 sessions the mice were accustomed to the operant box. During these sessions, the milk solution was delivered in the liquid trough at 1 min intervals. Reward was indicated by a brief tone and the illumination of a cue light mounted above the lever.

Fixed ratio training: Following the two habituation sessions, mice were trained to lever respond for the milk solution in 1h sessions under a fixed ratio 1 (FR1) schedule of reinforcement, in which each lever press leads to reward delivery. Sessions began with the illumination of the house light and the insertion of the levers inside the chamber. The animals were exposed to this schedule until achievement of the acquisition criterion of 200 lever responses per session.

Random ratio training: When the animals reached the acquisition criterion as described above, they were shifted to a random ratio (RR) schedule of reinforcement, in which lever-responses were reinforced with a given reward probability in order to increase the motivational demand of the task. The training consisted of three consecutive steps characterized by a different RR value that defined the probability of reinforcement [specifically RR 5 (p=0.2), RR 10 (p=0.1) and RR2 20 (p=0.05)]. Condition to move from one ratio to a higher one was the achievement of stable values of lever responses across 2 consecutive sessions.

Progressive ratio testing: In the progressive ratio PRx2 schedule, the number of lever presses required to earn a reward was doubled respective to the previous one obtained. Sessions were considered to be finished when the animal stopped lever-pressing for 3 min, allowing the

measurement of the session duration. Mice were tested multiple times in PRx2 with RR20 sessions intercalated between each PR tasks. For each animal, sessions of PRx2 were averaged, excluding the first ones that were consistently outliers.

Amphetamine was administered intraperitoneally 10 min before the beginning of the PRx2 test sessions. Amphetamine (Amph ; Merck) was dissolved in NaCl 0.9% and administered at 0.1mg/kg. In a first PRx2 session, half of the animals received saline, the other half received amphetamine. A second PRx2 session was performed 2 days later in which animals that received saline in the first PRx2 were then injected with amphetamine, and vice-versa. This allowed within-subject analyses in which the ratio of lever presses under drugs over lever presses after vehicle injection were measured for each animal and averaged in order to evaluate the effect of the drugs on operant responding.

Concurrent lever pressing/free feeding task: This task was adapted from a procedure designed by John Salamone (Salamone et al., 1991). Briefly, in this effort-based choice task the animals had the choice between lever pressing for the palatable milk reward under a RR20 schedule or consume the freely-available, though less-palatable, regular chow. Total lever presses and amount of concurrent food (mg) consumed were measured. Non-concurrent RR20 were intercalated between each concurrent session.

Licking microstructures

A home-made lickometer was used to record the licking microstructures in response to a palatable solution. The lickometer consisted of a testing chamber (20 cm wide, 30 cm deep, 15 cm tall), a bottle containing the solution connected to a dedicated computer (with a software that recorded the precise timing of each lick). All licks were recorded, and the short response latency provided a precise measure of the onset and offset of licks. Before testing, mice were first habituated to the experimental chamber for 2 days with free access to water during a 30 min-session. On the testing day, water was replaced by 10% sweetened condensed milk and each mouse was placed individually in the chamber for 30 min during which the amount of milk consumed, the number of licks and bursts, the number of licks per burst and burst duration were recorded (a burst is defined by an interlick interval lower than 0.25 seconds between each licks that compose it (Johnson, 2018).

Lipid analyses

Lipids and other material:

Chloroform ($CHCl_3$) was obtained from SDS (France). Ammonium acetate, acetonitrile (CH_3CN), methanol (CH_3OH) and water (H_2O) of Optima LC/MS grade were all from Fisher Scientific (France). Commercially available phospholipid (PL) standards were purchased from Avanti Polar Lipids INC-Coger (Paris, France).

Lipid extraction:

Total lipids were extracted, homogenized in H_2O, overnight at 4°C, with 10 volumes of $CHCl_3/CH_3OH$ (1:1, v/v). The residual pellets obtained after centrifugation (1500g, 5 min) were then re-extracted with 3 mL $CHCl_3/CH_3OH$ (1:1, v/v), 3 mL $CHCl_3/CH_3OH$ (2:1, v/v) and 3 mL $CHCl_3/CH_3OH/H_2O$ (48:35:10, v/v/v). The four lipid extracts were combined, and evaporated to dryness under a stream of nitrogen.

Fatty Acid distribution:

Fatty acid methyl esters were prepared for analysis by gas chromatography-flame ionization detection. Briefly, an aliquot of the total lipid extract was transmethylated using boron trifluoride in methanol according to Morrison and Smith (Morrison and Smith, 1964). Fatty acid methyl esters (FAMEs) were extracted with hexane and analyzed by gas chromatography ionization detector (GC-FID, Hewlett Packard HP5890, Palo Alto, CA). A 1µl aliquot was injected by automated injection in a splitless mode at an injection temperature of 250°C on a CPSIL-88 column (100 m × 0.25 mm i.d., film thickness 0.20 µm; Varian, Les Ulis, France) equipped with a flame ionization detector. Hydrogen was used as the carrier gas (inlet pressure 210 kPa). The oven temperature was held at 60°C for 5 min, increased to 165°C at 15°C/min and held for 1 min, and then to 225°C at 2°C/min and finally held at 225°C for 17 min. The detector was maintained at 250°C. FAMEs were identified by comparison with commercial and synthetic standards. The data were processed using the EZChrom Elite software (Agilent Technologies, Massy, France) and reported as a percentage of the total FAs.

Cholesterol analysis:

An aliquot of the total lipid extract (20 µg) was submitted to alkaline hydrolysis in 5 ml of 1 M KOH for 2 hr. submitted to alkaline hydrolysis in 5 ml of 1 M KOH for 2 hr. The solution was neutralized with 65 µL of phosphoric acid, and the sterols were extracted with 9 mL of chloroform in the presence of 3 mL of 0.9% sodium chloride. The organic phase was removed, and the solvent was evaporated to dryness. 3.25 µg of 5α-cholestane was added and sterols were derivatized to trimethylsilyl ethers by heating at 60°C after the addition of 200 µl of pyridine and 200 µl of BSTFA (Supelco, Bellafonte, PA, USA). The solvents were evaporated under nitrogen gas, and the samples were resuspended in hexane and analysed by GC-FID (Hewlett-Packard HP4890A, Palo Alto, CA). A

1µl aliquot was injected by automated injection in a splitless mode at an injection temperature of 300°C on a DB-5MS fused silica capillary column (30 m x 0.25 mm id, film thickness 0.25 µm; thickness; J&W Scientific, Agilent Technologies, Massy, France). The oven temperature was held at 50°C for 1 min, increased to 200°C at 20°C/min and then to 300°C at 5°C/min. The detector was maintained at 300°C. The data were processed using the EZChrom Elite software (Agilent Technologies, Massy, France)

Separation and quantification of phospholipid classes by liquid chromatography coupled to charged aerosol detector (CAD):

The phosphorus content of the total lipid extract was determined according to the method developed by Bartlett and Lewis (Bartlett and Lewis, 1970). The samples were then diluted to the appropriate concentration of 500 µg/µL of PLs in $CHCl_3$/CH_3OH (1:1, v/v). PLs were first separated by liquid chromatography under HILIC conditions and then detected using a Corona™ Ultra RS Charged Aerosol Detector™ (CAD, Thermo Scientific, USA). HPLC was performed using a Dionex UltiMate™ 3000 LC pump from Thermo Scientific (USA) equipped with a dual-gradient pump, which allows for a post-separation inverse gradient approach to compensate for solvent gradient effects in CAD detection. In this approach, a secondary stream of solvent is mixed with the column effluent such that the mixture of aqueous–organic eluent introduced into the detector inlet remains in equal proportions throughout the run. Separation of phosphatidylinositol (PI), phosphatidylethanolamine (PE), phosphatidylcholine (PC) and sphingomyelin (SM) standards was achieved under HILIC conditions using a Thermo Accucore column (150 x 2.1 mm, 2.6 µm, Hilic, Thermo Scientific, USA). The mobile phase consisted of (A) CH_3CN /H_2O (95:5, v/v) containing 5 mM ammonium acetate and (B) CH_3CN /H2O (50:50, v/v) containing 10 mM ammonium acetate. The solvent-gradient system of the analytical pump was as follows: 0 min 100% A, 1 min 95% A, 20 min 80% A, 23 min 65% A, 24 min 100% A and 24–39 min 100% A. The flow rate was 800 µL·min−1, the injection volume was 5 µL and the column was maintained at 40°C. Solvent gradient compensation was performed using the following inverse gradient program “minimize flow”, at a flow rate 280 µL.min-1: 0–1.786 min 100% B, 2.786 min 85.7% B, 21.786 min 42.9% B, 24.786 min 0% B, 25.786 min 100% B, 25.786-40.786 min 100% B. Eluate from the HPLC system was introduced into a CCAD for detection of the PLs. The settings for the CCAD were as follows: gas inlet pressure (nitrogen) 35 psi; gas flow rate and flow ratio 1.11 L/min and 0.95, respectively; corona voltage 2.9 kV; corona current and current range 1.0 µA and 100 pA, respectively; ion trapping voltage 20.4; filter “3”; data collection rate 10 Hz; power function 1.5; and nebulizer temperature 25°C. The liquid chromatography and the CAD were controlled by Chromeleon 7.2 (Thermo Scientific Dionex).

Structural analysis of phospholipids by liquid chromatography-mass spectrometry:

The structural analysis of PLs was performed using a LC-ESI-MS method according to previously described procedures (Acar et al., 2012; Berdeaux et al., 2010; Koehrer et al., 2014). The total lipids were dried under a stream of nitrogen. The samples were then diluted to the appropriate concentration of 12.5 ng/µL of PLs in $CHCl_3/CH_3OH$ (1:1, v/v) for analysis. The samples were stored at -80°C under an argon atmosphere.

LC was performed using a Dionex UltiMate™ 3000 LC pump from Thermo Scientific (San Jose, CA, USA) equipped with an autosampler. Separation of PL classes was achieved under hydrophilic interaction liquid chromatography (HILIC) conditions using an Accucore HILIC column (150 mm x 2.1 mm i.d., 2.6 µm, Thermo). The mobile phase consisted of (A) CH_3CN/H_2O (95:5, v/v) containing 5 mM of ammonium acetate and (B) CH_3CN /H_2O (50:50, v/v) containing 5 mM of ammonium acetate. The solvent-gradient system was as follows: 0 min A/B (%) 100/0, 1 min A/B (%) 95/5, 20 min A/B (%) 80/20%, 22 min A/B (%) 75/35 and 24-39 min A/B (%) 100/0. The flow rate was 400 µL.min−1, and the column was maintained at 30°C. The flow from LC was split using an analytical fixed flow splitter (split ratio = 1:1, post-column) from Analytical Scientific Instruments (El Sobrante, CA, USA). Mass spectrometry was performed using a ThermoFinnigan TSQ Quantum triple quadrupole mass spectrometer equipped with a standard electrospray ionization source outfitted with a 100-µm i.d. H-ESI needle. The source spray head was oriented at a 90° angle orthogonal to the ion-transfer tube. Nitrogen was used for both the sheath and the auxiliary gases. The MS signals of PC species were first optimized by continuous infusion of the standards dissolved in the mobile phase using ESI in the negative and positive modes. The electrospray ionization spray voltages were 3 kV and −4.5 kV in the negative- and positive-ion modes, respectively; the vaporizer temperature was 150°C; the sheath gas N2 pressure was 45 (arbitrary units); the auxiliary gas pressure was 45 (arbitrary units); the ion sweep gas pressure was 5; the ion transfer capillary temperature was 300°C; the skimmer offset was 5 V; and the multiplier gain was 300,000.

When operated under full-scan conditions in the negative- and positive-ion modes, data were collected in the range of m/z 400–1100 amu with a scan time of 0.5 sec. For PC characterization in the negative mode, ESI-MS/MS was used with argon as the collision gas at 1.5 mTorr, and the collision energy was set to 15 eV; in the positive mode, the collision gas pressure was 0.8 mTorr, and the collision energy ranged from 30 to 45eV. PE and PC species were manually identified with the parent mass information and their characteristic fragment ions in the collision-induced dissociation (CID) spectrum using lists of PL species prepared in our laboratory (Acar et al., 2012; Berdeaux et al., 2010).

Upon CID in the positive mode, PC, plasmenyl-choline (PlsC) and SM species showed an intense fragment at m/z 184 amu because of their common choline head group. This fragment at m/z 184 amu was used for precursor ion scanning, whereby the $[M+H]^+$ ions of PCs and SM are specifically detected. Upon CID in the positive mode, $[M+H]^+$ ions of PE lose their ethanolaminephosphate head group as a neutral fragment of 141 Da. Therefore, positive-ion-mode neutral loss scanning of 141 Da was used for the selective detection of PE.

The data were processed using the Xcalibur software (ThermoFinnigan). Corrections were applied to the data for isotopic overlap.

Slice preparation and whole-cell patch clamp recording

Mice were anaesthetized with isoflurane and dislocated. The brain was quickly removed and sagittal slices (350µm) were prepared with a vibratome (VT1000S, Leica) in 4°C artificial cerebrospinal fluid (aCSF) containing (in mM) 125 NaCl, 25 NaHCO3, 2.5 KCl, 1.25 NaH2PO4, 2 CaCl2, 1 MgCl2, 25 glucose and 1.25 pyruvate (oxygenated with 95% O2/5% CO2). After 60 min of recovery, slices were transferred to a recording chamber and perfused continuously at ≈ 1-1.5 mL/min with oxygenated ACSF, containing (in mM) 125 NaCl, 25 NaHCO3, 2.5 KCl, 1.25 NaH2PO4, 2 CaCl2, 1 MgCl2 and 25 glucose at room temperature. Cells were visualized with a water-immersion objective on an upright fluorescent microscope (Eclipse E600FN; Nikon Instruments) equipped with infrared-differential interference contrast video microscopy and epifluorescence. Patch pipettes (3-6 MΩ) were pulled from borosilicate glass (BF-150-86-10; Sutter Instruments) with a micropipette horizontal puller (P-97, Sutter Instruments) and filled with internal solutions.

Electrophysiological recordings were performed at room temperature using a MultiClamp700B amplifier (Molecular Devices) and acquired using a Digidata 1440A digitizer (Molecular Devices), sampled at 20 kHz for current clamp and 200 KHz for voltage-clamp recordings and cell-attached recordings, and filtered at 1 kHz. All data acquisitions were performed using pCLAMP 10.7 software (Molecular Devices). Stimulation of fibers from the frontal cortex was performed with a stimulating electrode (bipolar concentric electrode from Phymep and stimulator A365, World Precision Instruments). Only cells that maintained a stable access resistance (<30MΩ, no compensation) throughout the entire recording were included in analyses. In D1-EGFP mice, GFP-positive and negative MSNs were recording within the NAc core. For the pharmacogenetics experiments (D2-cre mice), recordings were restricted to mcherry-negative MSNs (putative D1-MSNs).

Cesium-chloride internal solution which consisted of (in mM) 150 CsCl, 2 MgCl2, 1 EGTA, 2 Na2-ATP, 0.2 Na-GTP, 0.2 cAMP, 10 HEPES, 0.2% neurobiotin pH 7.35 was used to record GABA-mediated

spontaneous inhibitory post-synaptic currents (sIPSC). They were recorded in the presence of 10 µM CNQX (6-cyano-7-nitroquinoxaline-2,3-dione, Merck) and 50 µM D-AP5 (D-2-amino-5-phosphonovalerate, Tocris) to block AMPA and NMDA receptors, respectively. When appropriate, the voltage-gated sodium channel antagonist tetrodotoxin (TTX, 1 µM, Tocris) was added to the perfusing solution in order to isolate miniature inhibitory postsynaptic currents (mIPSC) and Gabazine (Gbz, 5 µM, Tocris) was used in order to measure $GABA_A$ receptors-mediated tonic inhibition. In these cases, neurons were voltage clamped at -70 mV.

For recordings of basic intrinsic properties and EPSP/Spike coupling, we used the potassium-gluconate internal solution which consisted of (in mM) 128 KGlu, 20 NaCl, 1 MgCl2, 1 EGTA, 0.3 CaCl2, 2 Na2-ATP, 0.3 Na-GTP, 0.2 cAMP, 10 HEPES and 0.2% biocytine, pH 7.35. To record basic intrinsic properties of MSNs, cells were held in current-clamp mode in the absence of any current injections. A series of depolarizing current steps starting at -150 pA with 10 pA increment were then applied. For the spontaneous excitatory post-synaptic currents (EPSCs) recordings, neurons were clamped at -60mV. For the EPSP/Spike (E-S) coupling protocol, neurons were current clamped at -60 mV. The intensity of stimulation applied on glutamatergic afferents was from 50µA to 2000µA. For E–S coupling, the firing probability was plotted as a function of the EPSP slope based on a previously published study (Campanac and Debanne, 2008). EPSP slopes measured during the first 2.5ms and the percentage of spikes were determined by establishing a survival curve where, for each measured slope, a spike is considered as an event. The E–S shift for a firing probability of 50% was also analyzed to evaluate the drugs effect (Staff and Spruston, 2003). Data were analyzed offline using Clampfit (Molecular Devices).

For cell-attached recordings of spike frequency in VP neurons, we used filtered extracellular medium.

For pharmacological experiments, baseline responses were recorded and drugs were bath applied for 5 min (TTX 1µM to block neuronal activity, Gbz 5 µM to block inhibitory currents mediated by $GABA_A$ receptors; Quin [10µM, Tocris] to activate dopamine D2 receptors and Clozapine-N-Oxide [CNO, 10µM, Enzo] to activate hM4Di receptors).

Stereotaxic Surgeries for microdialysis

Mice were anesthetized with urethane (1 g/kg, i.p.) and placed in a stereotaxic apparatus (RWD life science) under body-temperature control. The probes (1 mm-long membranes, CMA 11, Phymep, France) were stereotaxically implanted into the left ventral striatum (vStr, bregma: 1.54 mm, lateral: 0.8 mm lateral, ventral: -4.7 mm ; Paxinos and Franklin, 2013). The probe was connected to an

infusion pump and perfused with Ringer's solution at 1µl/min (NaCl 142 mM, KCl 3.9 mM, $CaCl_2$ 1.2 mM, $MgCl_2$ 1 mM, Na_2HPO_4 1.35 mM, NaH_2PO_4 0.3 mM ; pH=7.35). The dialysates were collected at 20-min intervals after a 60 min washout period. The average concentration of dopamine in the first three dialysate samples was taken as baseline dopamine levels, followed by amphetamine injection (Amph 1mg/kg, i.p. ; Merck). Four more samples were then collected for a total of 2h and 20min of dialysate collection. The mice were sacrificed and the brains collected for further histological verification of the probe implantation.

High-Performance Liquid Chromatography

The dialysate samples were injected into a high-performance liquid chromatograph equipped with a 5 µm C18, 3 x 100 mm silica column (ACE, AIT, France) and a DECADE II detector (Antec Leyden, The Netherlands) to quantify dopamine. The mobile phase, consisting of 0.1 M acetate de sodium, 0.1 M citric acid, 1 M diéthylamine, 1.4 mM octanesulfonic acid and 0.1 mM EDTA, was pumped at 0.3 mL/min (Dionex SA, Voisins-Le-Bretonneux, France) through oxidation potential of the electrochemical detector (Decade 2, Antec, France) set at 600 mV. Signals were recorded and quantified with Chromeleon™ chromatography data system (Dionex SA, Voisins-Le-Bretonneux, France). DA concentration was calculated relative to a daily-injected standard. Results were expressed as a percentage of dopamine from baseline for each mouse.

Quantification of the relative projection density

Animals were anaesthetized and transcardially perfused with ice-cold 4% paraformaldehyde. Brains were harvested, postfixed overnight and washed in PBS. 100 µm sagittal thick sections were made on a vibratome and imaged using a macroscope Leica Z16 APO. Quantification of the relative projection density was achieved using the fluorescence intensity of the genetically encoded protein tdTomato in mice expressing this transgene under either the Drd2 (D2-Cre mice) or the Drd1 (D1-Cre mice) promoter. Red fluorescence intensity (in arbitrary units, a.u.) was measured in the dorsal part of ventral pallidum (VP), and nucleus accumbens (NAc) core. In each region, a region of equal size was drawn and the fluorescence intensity was quantified using ImageJ. The fluorescence intensity in the projection area region (VP) was normalized to the intensity in the corresponding NAc region ($^{VP}/_{NAc}$). Images of the striatal region and its corresponding projection region were taken from the same slice. Magnification was maintained between images (4x).

Western blot

Mice were dislocated and the brains were quickly removed and snap-frozen in isopentane (Merck) on dry ice and stored at -80°C. Nucleus accumbens samples were punched (No.18035-01, Fine Science Tools) from 200 µm frozen slices in a cryostat.

Samples were homogenized in 80 µl of denaturing buffer (DTT 2 mM, SDS 20%) containing protease and phosphatase inhibitors (No.13393126, Fisher Scientific) by a brief sonication. Protein content was determined by using the protein quantitation kit MicroBC assay (No.UP75860A, Interchim) according to the manufacturer's protocol (Interchim) and samples were then denatured at 90°C for 5 min, except for analysis of the D2 receptor for which denaturation was performed at room temperature.

Equal quantities of proteins (10µg/well) were separated by electrophoresis onto 10-12% polyacrylamide gels and then transferred on nitrocellulose membranes (Amersham Protan Premium 0.2µm). Membranes were saturated by incubation with 5% milk in Tris-Buffered Saline (TBS) and Tween 0.1% (Tris/HCl pH 7.5, NaCl 100 mM, Tween-20 0.1%) for 1h. Blots were probed overnight at 4 °C with primary antibodies (1:1000 rabbit anti-D2R, 1:1000 rat anti-D1R, 1:1000 rabbit anti-DAT, 1:5000 mouse anti-TH, 1:10000 mouse anti-tubulin; see resources table). After washes in TBS-Tween, membranes were incubated with the secondary antibody coupled to Horse Radish Peroxidase (HRP, 1/5000, Jackson ImmunoResearch) diluted in 5% milk in TBS-Tween, for 1h at room temperature. Membranes were washed and the complex was revealed with a West Dura Extended Duration Substrate (N°34075, ThermoFisher Scientific). Optical density capture of the signal was performed with the ChemidocMP imaging system (BioRad) and intensity of the signal was quantified using the Image Lab 5.2.1 software (BioRad).

Immunohistochemistry

Mice were transcardially perfused with ice-cold 4% paraformaldehyde in PBS under anesthesia. Brains were harvested, postfixed overnight and washed in PBS. 40 µm coronal sections were obtained using a vibratome and incubated in a blocking solution (10% fetal Bovine Serum in TBS: Tris 0.1M, NaCl 0.9%, pH 7.4) for 2h at room temperature. Slices were labeled overnight at 4 °C with primary antibodies against Cre recombinase (rabbit; 1:5, provided by Dr. C. Kellendonk ; see resources table) in D2- and D1-cre mice allowing colocalisation with the tdTomato Cre-dependent reporter. Other slices from D2-cre DREADD-transduced mice were labeled with primary antibodies against VAChT (rabbit, 1:1000, Synaptic System; see resources table) to label cholinergic interneurons. Sections were incubated with fluorescent secondary antibodies for 2h at RT and then mounted on slides and coverslipped with the fluorsave reagent (FluorSave™ Reagent, Cat.N°345789,

Merk Millipore). Digital images were acquired using a Leica SP1 confocal microscope, and processed with NIH Image J software.

Quantitative real-time PCR (q-PCR)

Prefrontal cortex, thalamus, hippocampus, striatum (dissection from fresh tissue or punches from snap-frozen brain tissue), liver, pancreas, gut and peri-gonadal fat tissues samples were homogenized in Tri-reagent (Euromedex, France) and RNA was isolated using a standard chloroform/isopropanol protocol (Chomczynski and Sacchi, 2006). RNA was processed and analyzed following an adaptation of published methods (Bustin et al., 2009). cDNA was synthesized from 2 µg of total RNA using RevertAid Premium Reverse Transcriptase (Fermentas) and primed with oligo-dT primers (Fermentas) and random primers (Fermentas). QPCR was perfomed using a LightCycler® 480 Real-Time PCR System (Roche, Meylan, France). QPCR reactions were performed in duplicate for each sample, using transcript-specific primers, cDNA (4 ng) and LightCycler 480 SYBR Green I Master (Roche) in a final volume of 10 µl. The PCR data were exported and analyzed in an informatics tool (Gene Expression Analysis Software Environment) developed at the NeuroCentre Magendie (Bordeaux, France). For the determination of the reference gene, the Genorm method was used (Livak and Schmittgen, 2001). Relative expression analysis was corrected for PCR efficiency and normalized against two reference genes. The glyceraldehyde-3-phosphate dehydrogenase (GAPDH), the Actin Beta (Actb), the Non-POU domain-containing octamer-binding protein (Nono) and the peptidylprolyl isomerase A (Ppia) genes were used as reference genes (among a total of 12 candidates). The relative level of expression was calculated using the comparative ($2^{-\Delta\Delta CT}$) method (3). Primers sequences are reported in resources table.

Stereotaxic Surgeries for viral injections

Stereotaxic injections of viral vectors were performed with a stereotaxic apparatus (RWD life science) under constant isoflurane anesthesia and i.p. buprenorphine and tolfedine for analgesia and inflammation. Mice were injected bilaterally with pAAV-hSyn-DIO-hM4D(Gi)-mCherry (0.5µl at titer > $4x10^{12}$ vg/ml; Cat.No.: 44362-AAV8, AddGene) in the Nucleus accumbens core (NAc core, bregma: 1.6 mm, lateral: 1 mm, ventral: -4mm; Paxinos and Franklin, 2013) using a 10 µL Hamilton syringe (Hamilton) and an ultra-micro pump (UMP3, World Precision Instruments, USA) at 150 nL/min. The injection needle was withdrawn 5 min after the end of the infusion. The incision was closed with a suture and the animal was kept on a heating pad until recovery. Experiments were performed 5-8 weeks after AAV stereotaxic injection. Injection sites were confirmed in all animals by preparing sagittal sections (350µm) for electrophysiological experiments.

Quantification and statistical analysis

Student's t tests (unpaired and paired) or equivalent non-parametric tests when normality failed (Mann-Whitney and Wilcoxon matched-pairs signed rank test) were used when two groups were compared. Welch's correction was applied on unpaired t-test when variances were not shown as equal. One sample t test was used to evaluate the effect of drugs on a variable before and after injection (Amphetamin PRx2 and Gabazine tonic inhibition). Log rank Mantel Cox test was used to compare survival curves obtained from PRx2 survival and E-S coupling experiments. Two-way ANOVA test was used when 2 factors were present (Two-way repeated measure ANOVA when one of the factors was a repeated measure). Bonferroni's post hoc test was applied when ANOVA showed a significant interaction or a significant main effect. All statistical data were obtained using GraphPad Prism 7 (Graphpad Software). Statistical significance was $^{\#}$ $p<0.1$, * $p < 0.05$, ** $p < 0.01$, *** $p < 0.001$. All data are presented as means ± SEM. Details of the statistical analysis per figure are summarized in tables S5 and S6 (main and supplemental figures respectively).

Data and code availability

The lipidomic datasets supporting the current study are available from the corresponding author on request.

Table S2 (Related to Fig. 1): Summary of brain lipidomic analysis

Table S3 (Related to Fig. 3-4): Summary of striatal lipidomic analysis

Table S5 (Related to Fig. 1-7): Summary of statistical analysis

Table S6 (Related to Fig. S1-7): Summary of supplemental statistical analysis

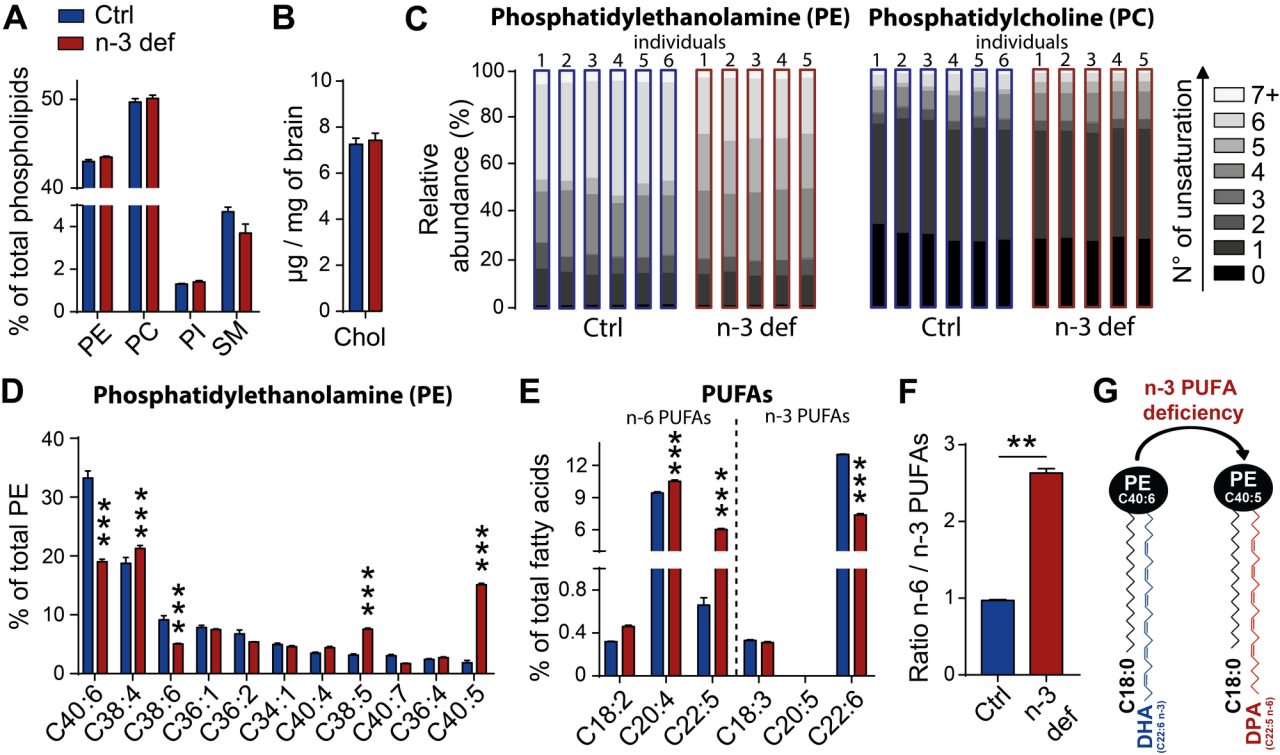
A
Ctrl
n-3 def
% of total phospholipids
PE
PC
PI
SM
B
µg / mg of brain
Chol
C
Phosphatidylethanolamine (PE)
Phosphatidylcholine (PC)
individuals
Relative abundance (%)
Ctrl
n-3 def
N° of unsaturation
7+
6
5
4
3
2
1
0
D
Phosphatidylethanolamine (PE)
% of total PE
C40:6
C38:4
C38:6
C36:1
C36:2
C34:1
C40:4
C38:5
C40:7
C36:4
C40:5
E
PUFAs
n-6 PUFAs
n-3 PUFAs
% of total fatty acids
C18:2
C20:4
C22:5
C18:3
C20:5
C22:6
F
Ratio n-6 / n-3 PUFAs
Ctrl
n-3 def
G
n-3 PUFA deficiency
PE C40:6
PE C40:5
C18:0
DHA (C22:6 n-3)
C18:0
DPA (C22:5 n-6)

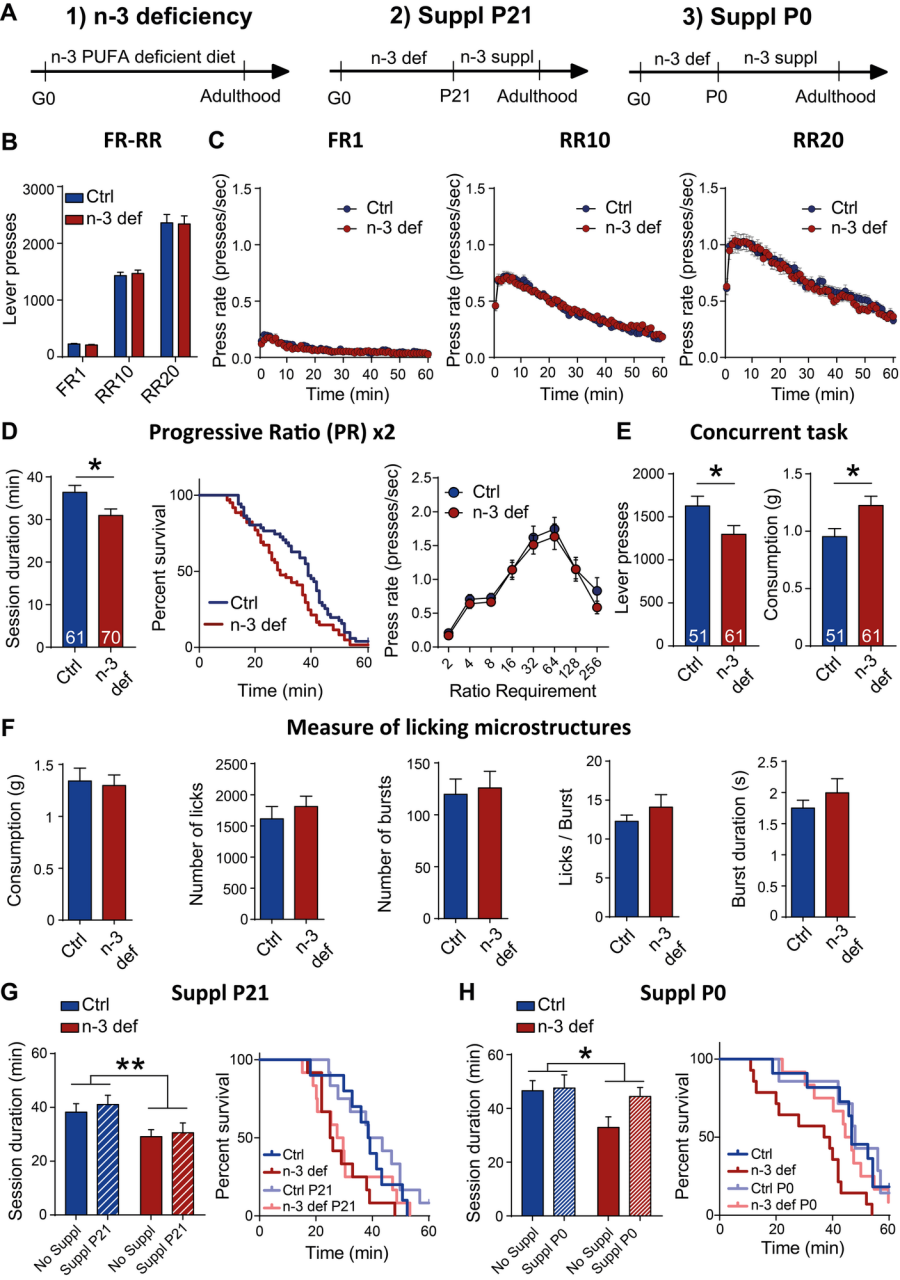
A
1) n-3 deficiency
n-3 PUFA deficient diet
G0
Adulthood
2) Suppl P21
n-3 def
n-3 suppl
G0
P21
Adulthood
3) Suppl P0
n-3 def
n-3 suppl
G0
P0
Adulthood
B
FR-RR
Ctrl
n-3 def
Lever presses
FR1
RR10
RR20
C
FR1
RR10
RR20
Ctrl
n-3 def
Press rate (presses/sec)
Time (min)
D
Progressive Ratio (PR) x2
Session duration (min)
Percent survival
Press rate (presses/sec)
Ratio Requirement
E
Concurrent task
Lever presses
Consumption (g)
F
Measure of licking microstructures
Consumption (g)
Number of licks
Number of bursts
Licks / Burst
Burst duration (s)
G
Suppl P21
No Suppl
Suppl P21
Ctrl P21
n-3 def P21
H
Suppl P0
Ctrl P0
n-3 def P0

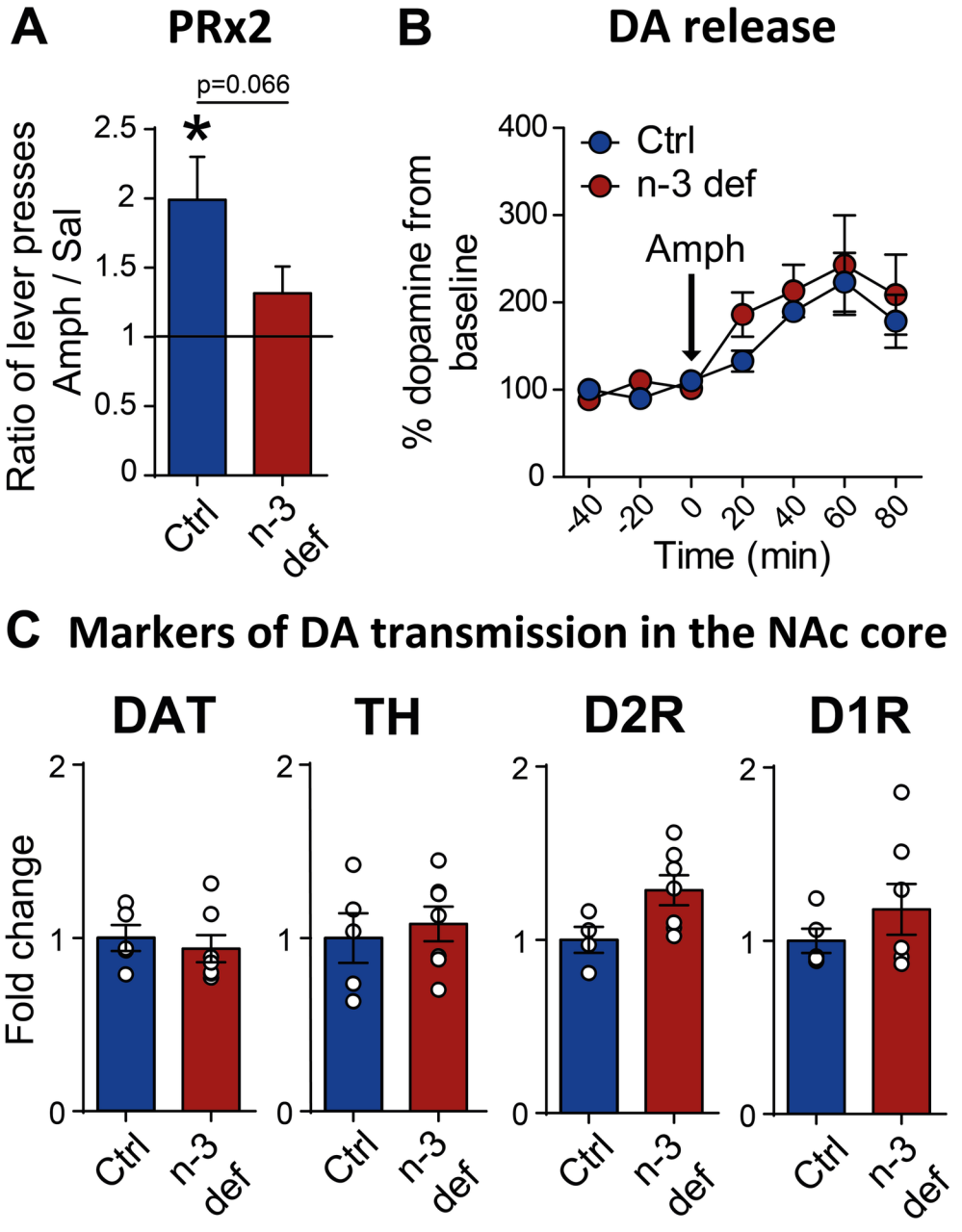
A
PRx2
p=0.066
*
Ratio of lever presses
Amph / Sal
2.5
2
1.5
1
0.5
0
Ctrl
n-3 def
B
DA release
% dopamine from baseline
400
300
200
100
0
Ctrl
n-3 def
Amph
-40
-20
0
20
40
60
80
Time (min)
C
Markers of DA transmission in the NAc core
DAT
TH
D2R
D1R
Fold change
2
1
0
Ctrl
n-3 def

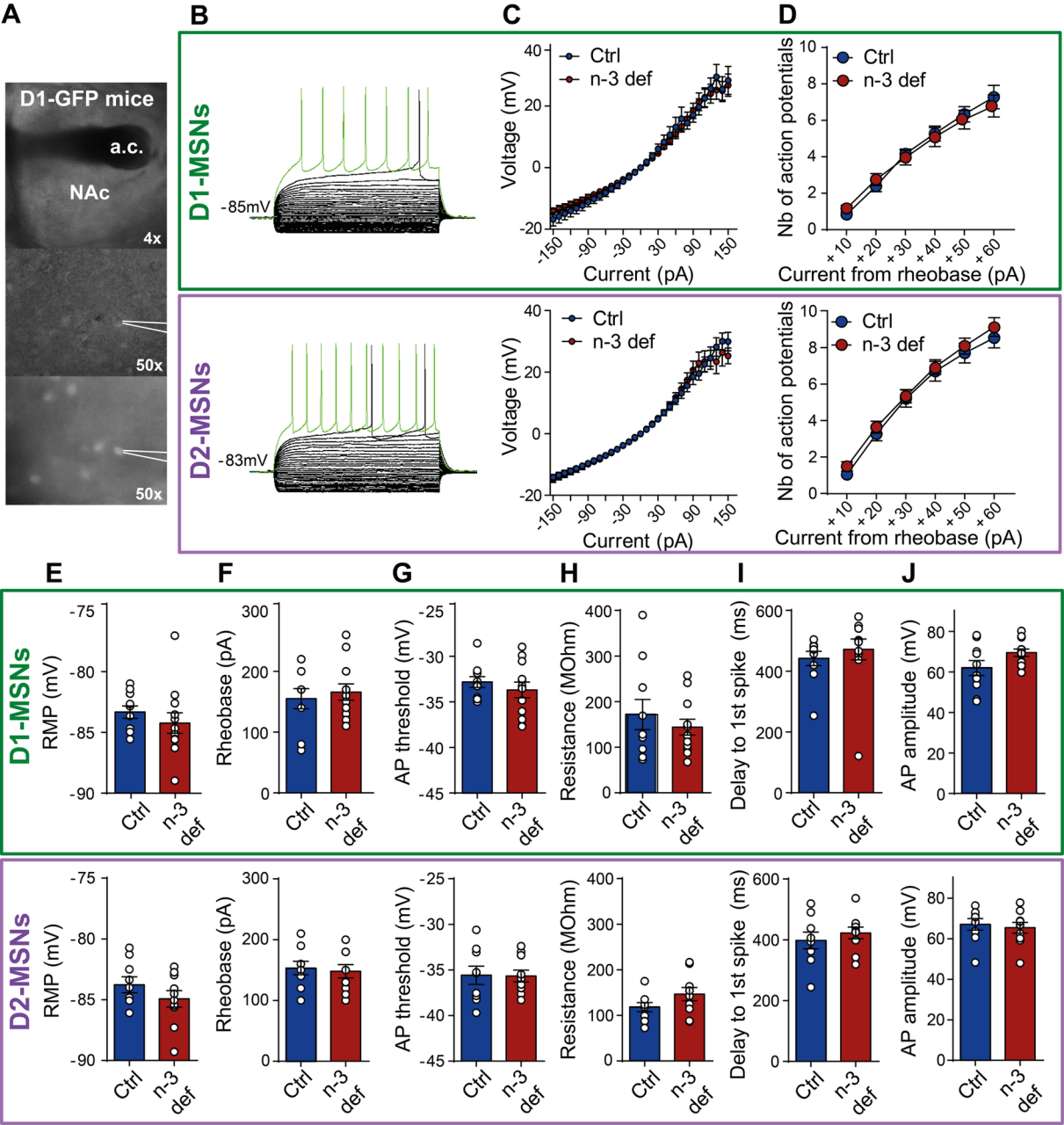
A
B
C
D
D1-GFP mice
a.c.
NAc
4x
50x
50x
D1-MSNs
-85mV
Ctrl
n-3 def
Voltage (mV)
Current (pA)
Nb of action potentials
Current from rheobase (pA)
D2-MSNs
-83mV
E
F
G
H
I
J
RMP (mV)
Rheobase (pA)
AP threshold (mV)
Resistance (MOhm)
Delay to 1st spike (ms)
AP amplitude (mV)

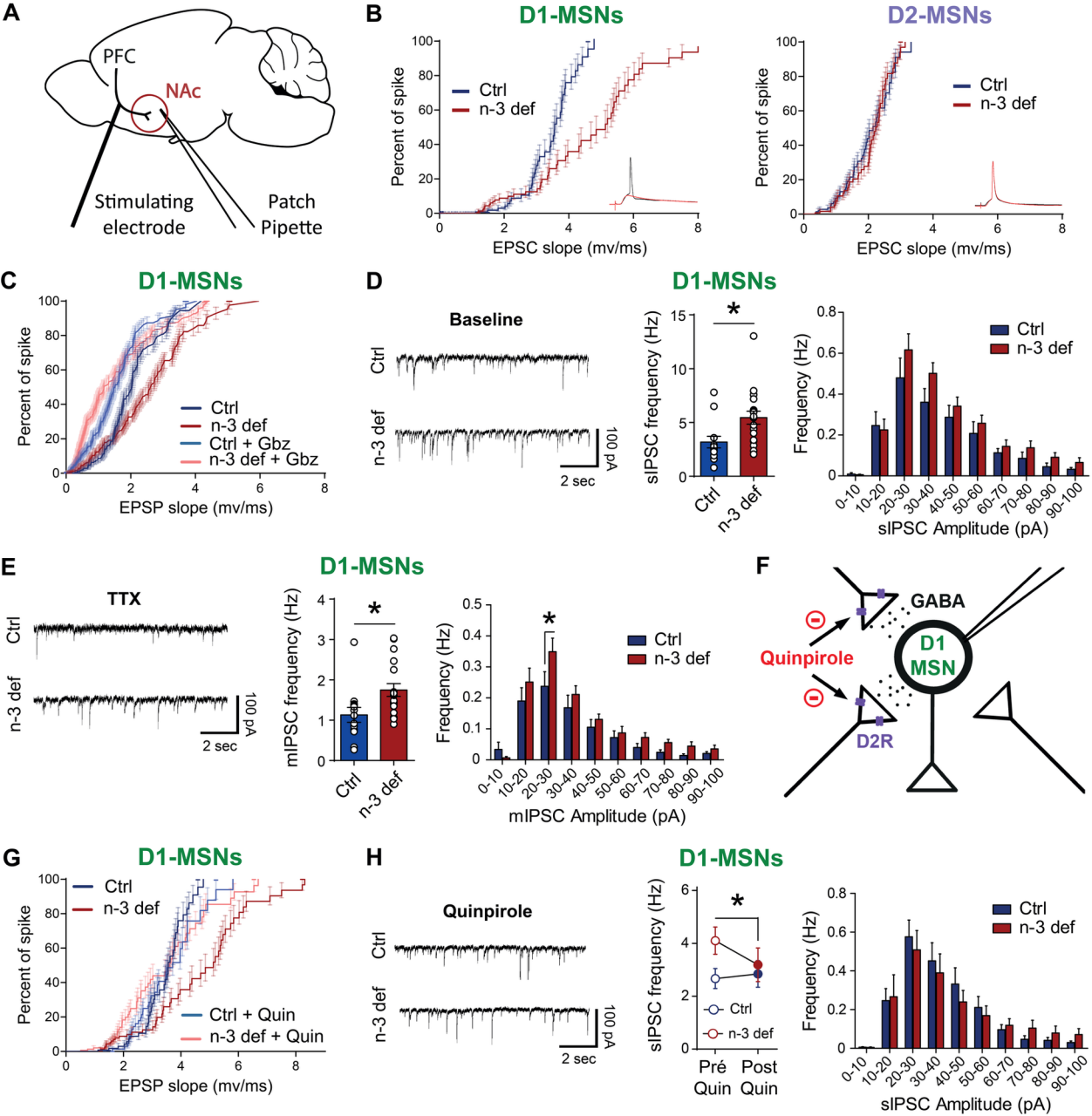
A
PFC
NAc
Stimulating electrode
Patch Pipette
B
D1-MSNs
D2-MSNs
Percent of spike
Ctrl
n-3 def
EPSC slope (mv/ms)
C
D1-MSNs
Ctrl + Gbz
n-3 def + Gbz
EPSP slope (mv/ms)
D
D1-MSNs
Baseline
100 pA
2 sec
sIPSC frequency (Hz)
Frequency (Hz)
sIPSC Amplitude (pA)
E
TTX
mIPSC frequency (Hz)
mIPSC Amplitude (pA)
F
GABA
Quinpirole
D1 MSN
D2R
G
D1-MSNs
Ctrl + Quin
n-3 def + Quin
H
D1-MSNs
Quinpirole
Pré Quin
Post Quin

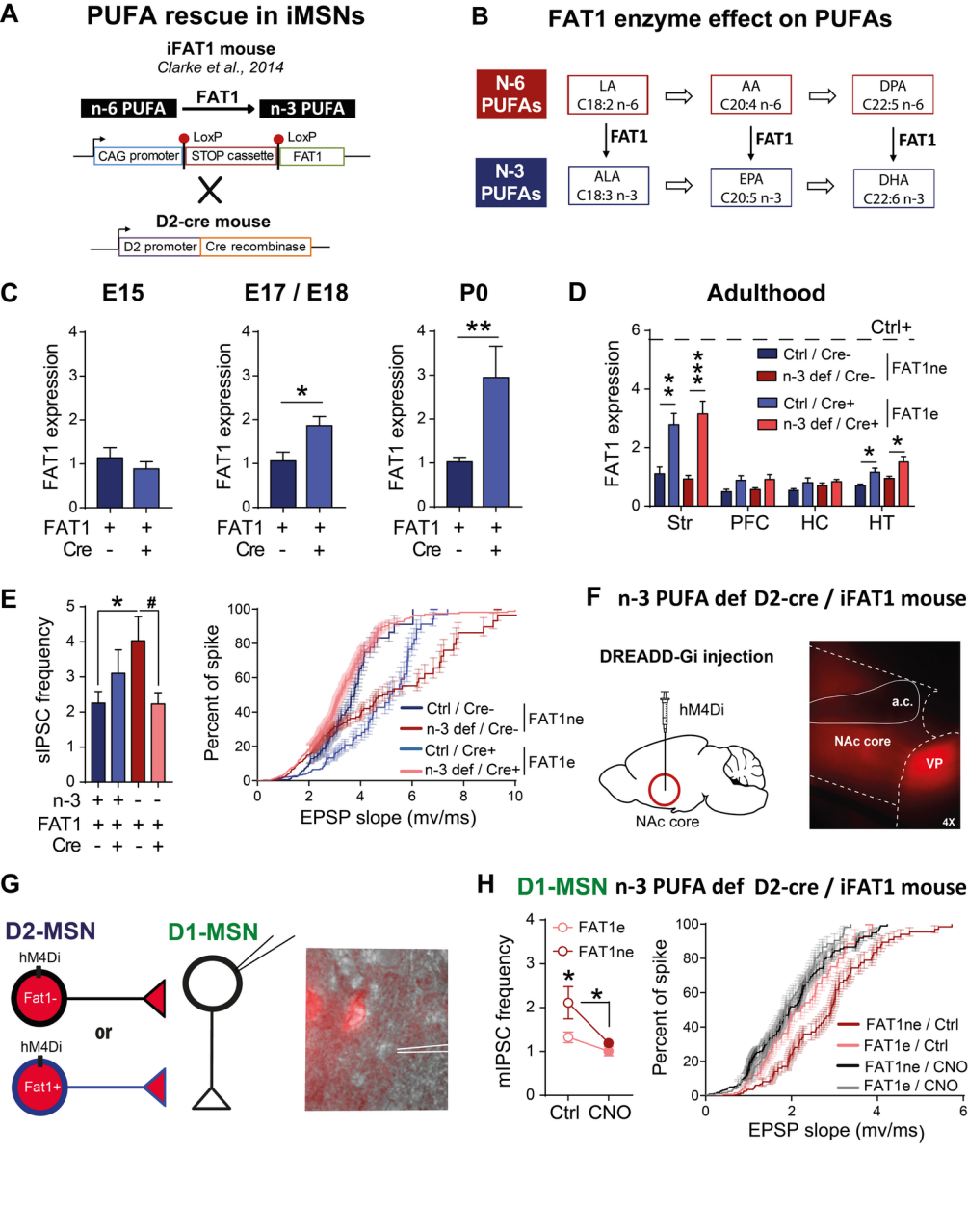
A
PUFA rescue in iMSNs
iFAT1 mouse
Clarke et al., 2014
n-6 PUFA
FAT1
n-3 PUFA
LoxP
LoxP
CAG promoter
STOP cassette
FAT1
D2-cre mouse
D2 promoter
Cre recombinase
B
FAT1 enzyme effect on PUFAs
N-6 PUFAs
LA C18:2 n-6
AA C20:4 n-6
DPA C22:5 n-6
FAT1
FAT1
FAT1
N-3 PUFAs
ALA C18:3 n-3
EPA C20:5 n-3
DHA C22:6 n-3
C
E15
E17 / E18
P0
FAT1 expression
FAT1 + +
Cre - +
D
Adulthood
Ctrl+
Ctrl / Cre-
n-3 def / Cre-
FAT1ne
Ctrl / Cre+
n-3 def / Cre+
FAT1e
Str
PFC
HC
HT
E
sIPSC frequency
n-3 + + - -
FAT1 + + + +
Cre - + - +
Percent of spike
EPSP slope (mv/ms)
Ctrl / Cre-
n-3 def / Cre-
FAT1ne
Ctrl / Cre+
n-3 def / Cre+
FAT1e
F
n-3 PUFA def D2-cre / iFAT1 mouse
DREADD-Gi injection
hM4Di
NAc core
a.c.
NAc core
VP
4X
G
D2-MSN
D1-MSN
hM4Di
Fat1-
or
hM4Di
Fat1+
H
D1-MSN n-3 PUFA def D2-cre / iFAT1 mouse
FAT1e
FAT1ne
mIPSC frequency
Ctrl CNO
Percent of spike
EPSP slope (mv/ms)
FAT1ne / Ctrl
FAT1e / Ctrl
FAT1ne / CNO
FAT1e / CNO

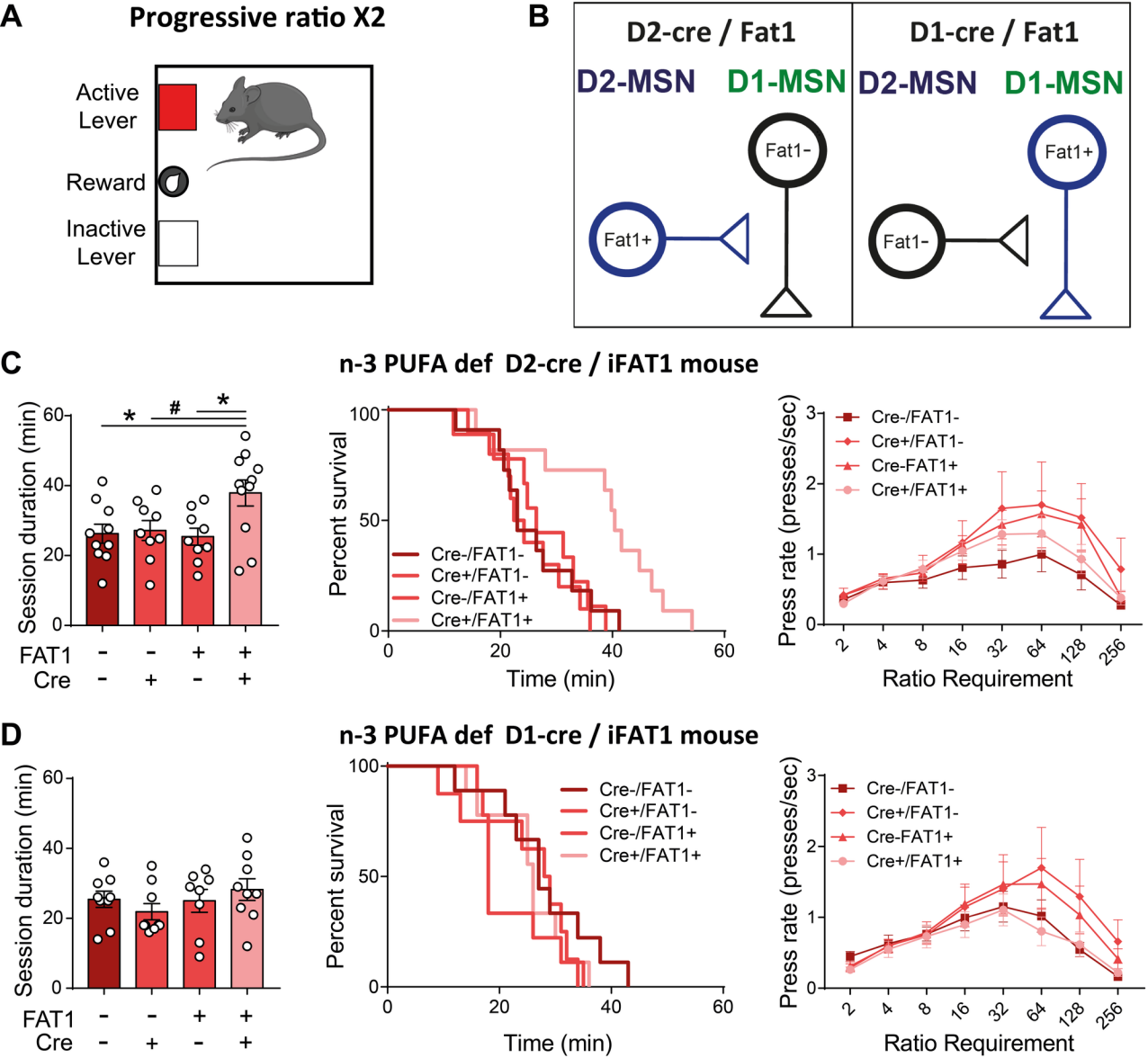
A
Progressive ratio X2
Active Lever
Reward
Inactive Lever
B
D2-cre / Fat1
D2-MSN
D1-MSN
Fat1-
Fat1+
D1-cre / Fat1
D2-MSN
D1-MSN
Fat1+
Fat1-
C
n-3 PUPA def D2-cre / iFAT1 mouse
Session duration (min)
FAT1
Cre
Percent survival
Time (min)
Cre-/FAT1-
Cre+/FAT1-
Cre-/FAT1+
Cre+/FAT1+
Press rate (presses/sec)
Ratio Requirement
D
n-3 PUPA def D1-cre / iFAT1 mouse
Session duration (min)
FAT1
Cre
Percent survival
Time (min)
Cre-/FAT1-
Cre+/FAT1-
Cre-/FAT1+
Cre+/FAT1+
Press rate (presses/sec)
Ratio Requirement

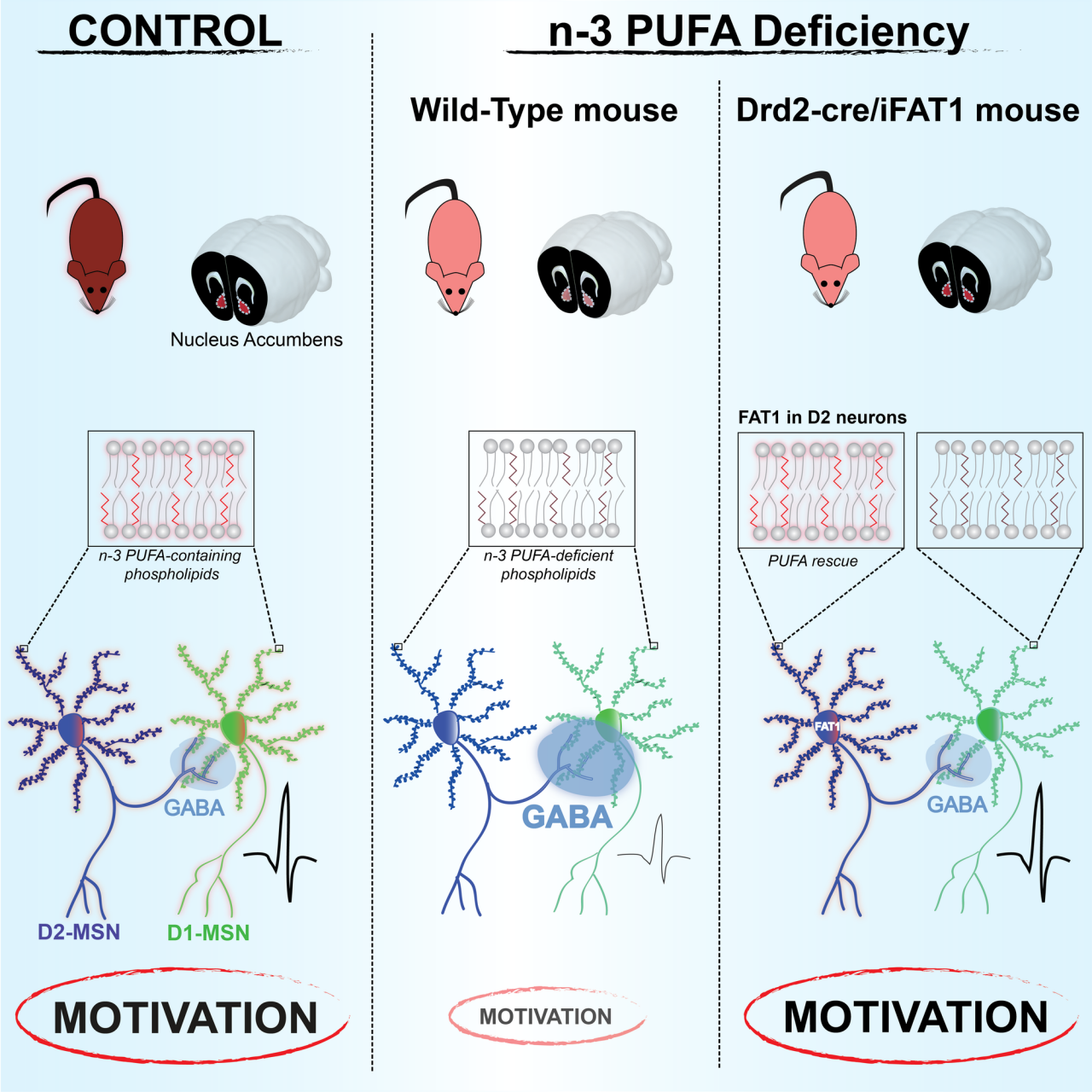
CONTROL
n-3 PUFA Deficiency
Wild-Type mouse
Drd2-cre/iFAT1 mouse
Nucleus Accumbens
n-3 PUFA-containing phospholipids
n-3 PUFA-deficient phospholipids
FAT1 in D2 neurons
PUFA rescue
FAT1
GABA
GABA
GABA
D2-MSN
D1-MSN
MOTIVATION
MOTIVATION
MOTIVATION